# Electromagnetic Interference Shielding For Solid Rocket Motors- Missiles


**By**

**Zahid Murtaza**

**School of Chemical and Materials Engineering**
**National University of Sciences and Technology**
**2020**

# Electromagnetic Interference Shielding For Solid Rocket Motors- Missiles

Name: Zahid Murtaza

Reg. No: 278699

**This thesis submitted as a partial fulfilment of the degree requirements for the degree of**

**MS in Energetic Materials Engineering**
**Supervisor Name: Dr. Sarah Farrukh**

**School of Chemical and Materials Engineering (SCME)**
**National University of Sciences and Technology (NUST)**
**H-12, Islamabad, Pakistan**
**Oct, 2020**

# Dedication

I dedicate this work to my parents, family, teachers and Pak Navy for their unflinching support and confidence in my abilities that enable me to perform my MS Degree in given time.

# Acknowledgements

All praise belongs to Allah Almighty, the beneficent, the merciful, for providing me the strength, courage and willpower to complete my work in time allocated to me.

I consider myself highly fortunate to have my supervisor like, **Dr. Sarah Farrukh**, whose able guidance and unflinching support helped me to perform all tasks in my research efficiently and timely. I owe a huge debt of gratitude to my respected co. supervisor **Dr. Abdul Qadeer Malik** and my guidance examination committee comprising of **Dr. Iftikhar Hussain Gul** and **Dr. Malik Adeel Umer,** for their valuable advice and kind guidance in my project.

I would like to appreciate all the lab facilities of NUST and Strategic organization for testing and characterization of samples necessary in accomplishment of project. I am immensely gratified to my family and Pak Navy for being the source of endless support and encouragement for me to complete my work.

# Abstract

Electromagnetic interference shielding has been used extensively in various electrical equipments to avoid interference due to Electrical and Magnetic fields. The Electromagnetic (EM) waves are the original source of EM interference and affect the life of expensive electronic assemblies. Electromagnetic interference shielding materials, used initially were usually metals that attenuate EM waves due to reflection phenomenon, but huge drawback for using metals as EMI Shielding purpose was their heavy structures and cost. Later, for development of electromagnetic interference shielding materials, various polymers were considered due to their properties of corrosion resistant, longer life time, less weight, specific stiffness, high strength, and ease in manufacturing. This research has primary focus on development of light weight polymer based EMI shielding material that can be economical, reliable and useful in terms of cost and benefit analysis for Military applications. Therefore, an EMI shielding material based on poly ethylene terephthalate (PET) polymer was selected due to its availability in abundance, thermal strength and economical nature. Further, PET nanocomposite based on hexagonal boron nitrate Nano sheets was also fabricated for enhanced tensile strength. This research depicted that both the PET and PET nanocomposite possess properties of absorption and reflection of EM wave respectively for attenuation of EMI. However, PET nanocomposites exhibited better tensile strength as well as shielding effectiveness in 2-18 GHz frequency range. The upshot of this research work is that PET nanocomposites are considered suitable option for EMI shielding.

# Table of Contents

# LIST OF FIGURES

# LIST OF TABLES

# List of Acronyms

| | |
|---|---|
| EMI | Electromagnetic interference |
| PET | Poly ethylene terephthalate |
| HBNNS | Hexagonal boron nitrate Nano sheets |
| NMP | N-methyl-2-pyrrolodine |
| DB | Decibel |
| GNP | Graphene Nano platelets |
| CNT | Carbon Nanotubes |
| SE | Shielding effectiveness |
| SE(R) | shielding effectiveness due to reflection |
| SE(A) | Shielding effectiveness due to absorption |
| SE(M) | Shielding effectiveness due to multiple reflection |
| SEM | Scanning electron microscopy |
| AFM | Atomic force microscopy |
| VNA | Vector network analyzer |

# Chapter 1
# Introduction

The increase in packing density of electronic assemblies in a single equipment for enhancing speed and size, causes a phenomenal increase in Electromagnetic Interference (EMI) within commercial mobile sets, LCDs, laptops [1].The EMI signals are unwanted distortions that occur in any electronic or military standard equipment and responsible for degradation of system performance, speed, reliability and life [2].Due care of EMI signals is essential for electrostatic discharge(ESD), safety of equipment and health hazards for human beings[3-5].Filtration of signals from nearby equipment, avoiding malfunctioning of electronic assemblies either military or commercial and resolving health problems like insomnia , headache requires shielding against these unwanted EM waves [6]. Effectiveness of EMI shielding materials usually measured in terms of reflection loss, absorption loss and multiple reflection losses and attenuation of incident Electromagnetic waves. These shielding materials upon exposure to incident EM wave nullify the intensity of incidence, either by reflection (due to mobile charge carrier electrons or holes) absorption (attenuation of EM waves by electric and magnetic dipoles) or multiple reflection (internal reflection caused by material due to porous or irregular structures).The EMI Shielding materials uses any of above phenomenon i.e. reflection, absorption or multiple reflection for suppression of unwanted EM wave to keep functionality, performance and reliability of electronic equipment as per standards. Fabrication of reflective, absorbent or multiple reflective material is different. Usually conductive metals are used for achieving reflective properties of materials, whereas magnetic materials gives better absorbing characteristics and porous, hollow and irregular materials give better multiple reflection for attenuation of EM waves. Initially, use of metals were in practice for EMI shielding of expensive electronic gadgetries but they lack application due to properties like stiffness, high cost and heavy weights. Later, researchers shown their interest towards polymer based EMI shielding materials due to their high performance, flexibility, corrosion resistance and lighter structures [7-11].

## 1.1. Electromagnetic Wave

Electromagnetic (EM) waves are basically the combination of both electric and magnetic fields and their propagation is perpendicular to both these fields, which are right angle to each other. EM wave is different to any other wave as it can propagate through any medium solid, air, water and vacuum with a reference speed of $3x10^8$m/s in vacuum. Figure. 1 show the vector representation of EM wave.

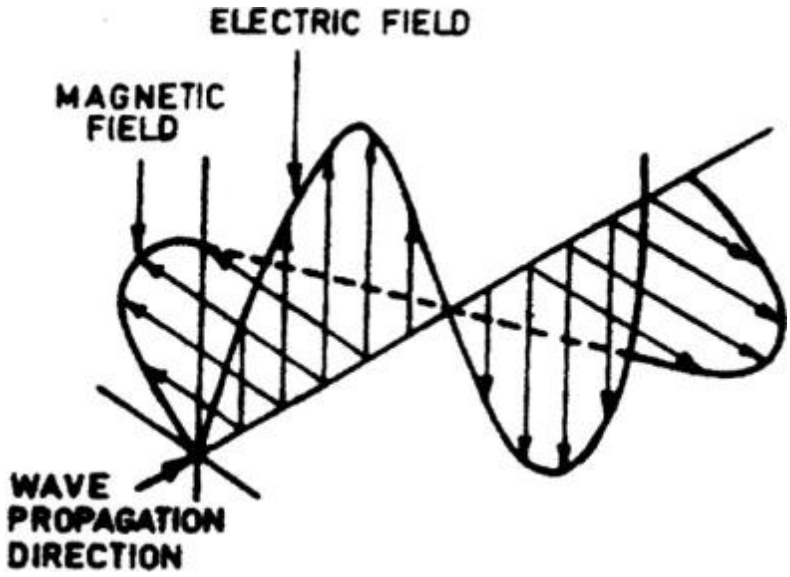


**Figure 1: Electromagnetic radiation vector**

Human activities have huge dependence on EM waves being the form of energy, its usage is not limited only to electricity (for house hold activities) but also its importance is inescapable in every sphere of life, whether medical (X-Rays), global positioning (Navigation), mobile communication (Radio frequency). EM wave is distributed in wide spectrum according to their frequencies or wavelengths. Radio waves and microwaves possess low frequencies but have longer wavelength for transmission, whereas X-Rays and Gamma Rays possess higher frequencies (shorter Wavelengths). Figure.2 show the entire EM wave spectrum [12].

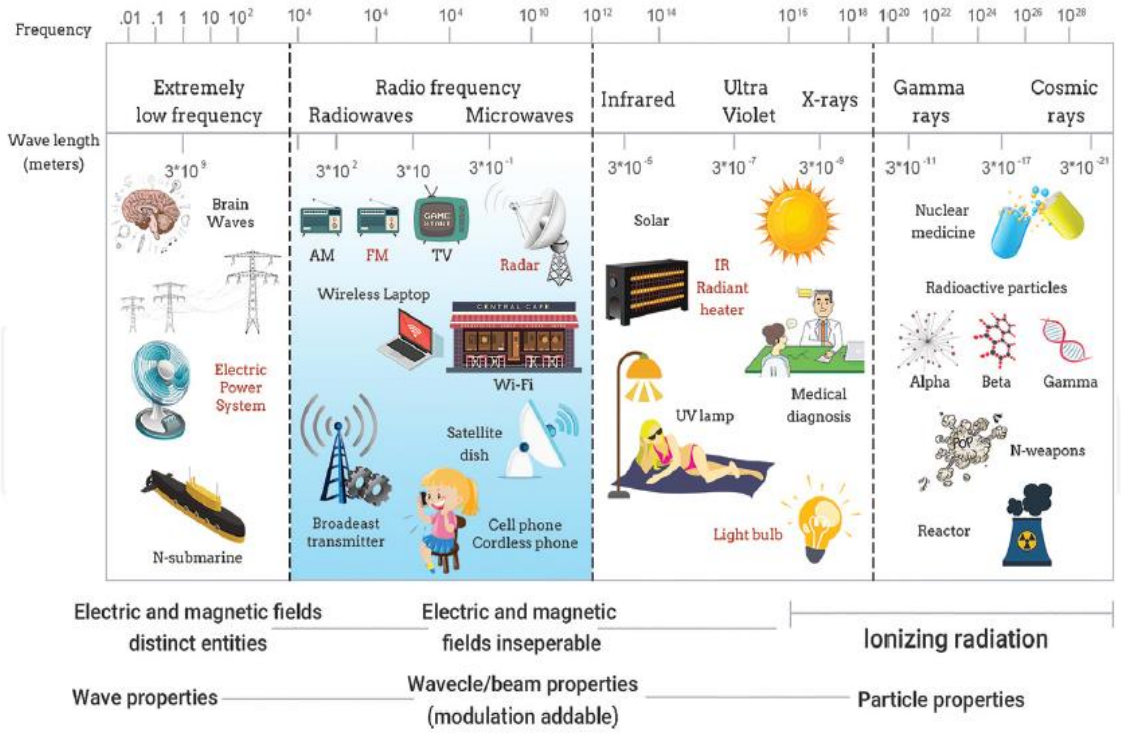


**Figure 2: EM spectrum properties across various ranges of frequencies and wavelengths**

## 1.2. Electromagnetic Interference Shielding

EMI capability of material is defined as a measure that how efficiently a material resists the EM wave of certain frequency passing through that material. It is the ratio between the input power (Pi) and output power ($P_0$) of a particular EM wave [13] as:

$$SE = 10 \log\left(\frac{pi}{po}\right) \qquad (Eq\ 1)$$

Unit of shielding effectiveness is given in decibels (dB). Further, relation of % attenuation of EM waves at specific value of shielding effectiveness (SE) in dB is represented in table-1 below:

**Table 1: Shielding effectiveness related with Attenuation %**

| SE (dB) | 20 | 30 | 40 | 50 | 60 | 70 |
|---|---|---|---|---|---|---|
| Attenuation % | 99 | 99.9 | 99.99 | 99.999 | 99.9999 | 99.9999 |

## 1.3. Near and far field condition of EM wave

Most important parameter of any EM wave is the wave impedance (Z), which is classified into two categories either near field or far field wave impedance. Further, it is directly depending on the distance (R) b/w the radiating source and shielding material or relative to total wavelength (λ) of the EM wave .The region within the distance R >λ/2 is considered as far field condition and R <λ/2 is adjudged as near field condition of EM wave as shown in the figure:

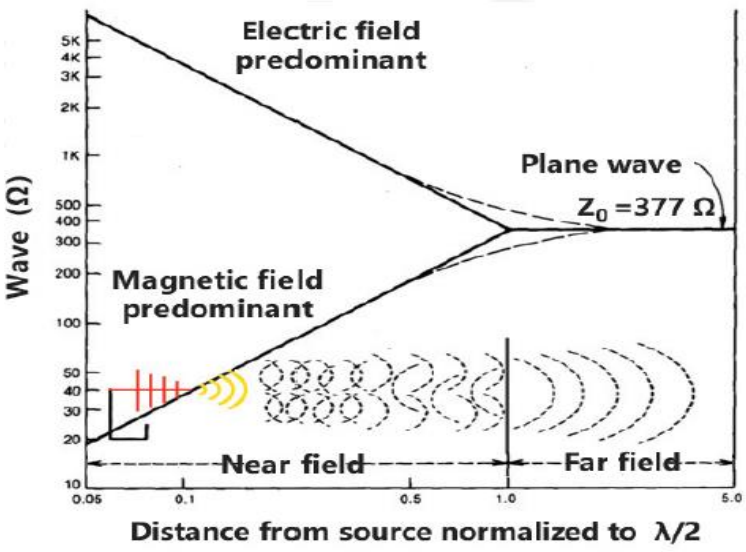


**Figure 3: Wave impedance in far field and near field [14]**

For EMI shielding materials, we always consider the far field condition b/c anything above the distance of 48cm and operating frequency of 100MHz is considered as far field condition and as for as the EMI shielding material is concerned, both the distance and frequency exceeds the pre requisite condition of far field condition. Hence, using far field condition, Electric field (E) and Magnetic field (H) effects are considered with EM wave to be regarded as plane wave. Therefore, following conditions need to be fulfilled:

$$Z = \frac{E}{H} \qquad (Eq\ 2)$$

$$E \perp H \qquad (Eq\ 3)$$

Where:

Z= Intrinsic Impedance or Wave Impedance

E=Electric field

H=Magnetic field

In case for Air, $\delta = 0$ (Electrical conductivity) $\mu=\mu_0$ (Relative permeability), $\varepsilon=\varepsilon_0$ (permittivity), the wave impedance $z_o$ equal to 377Ω and can be expressed as:

$$Zo = \sqrt{\frac{j\omega\mu}{\delta+j\omega\varepsilon}} = \sqrt{\frac{j\omega\mu o}{j\omega\varepsilon}} = \sqrt{\frac{\mu o}{\varepsilon o}} = 377\Omega \quad (Eq\ 4)$$

Where:

$\mu_0 = 4\Pi x\ 10^{-7}\ H/M$

$\varepsilon_0 = 8.85X10^{-12}\ F/M$

In the near field condition, wave front is considered as curved instead of planar so wave front is not parallel to shielding material. Therefore, wave impedance (Z) is different depending upon the dominance of Electric or Magnetic field. For dominant Electric field, the wave impedance decreases as the distance (R) increases but usually the wave impedance is greater than 377Ω and is expressed as [14]:

$$Z0 = \frac{1}{2\Pi f \varepsilon r} \quad (Eq\ 5)$$

For magnetic radiating source, the impedance is normally less than 377Ω and increases with increase in distance(R) and can be represented in the form as [14]:

$$Z0 = 2\Pi f \mu r \quad (Eq\ 6)$$

## 1.4. Reflection, Absorption and Multiple reflection phenomenon on Material shapes

EM wave travelling through any medium upon incident on material behave differently due to shape, size, structure and composition. However, three different processes namely reflection loss, absorption loss and multiple reflection loss assists in attenuation of EM wave and corresponds to shielding effectiveness(SE) in term of SE(R), SE(A) and SE(M) respectively. Figure 4(a-g) below depicts the possible interaction of EM waves with different materials. Figure 4(a) represents the schematic diagram of incident power, reflected power and transmitted power and electromagnetic field intensities of incident EM wave on a 3D material. Figure 4(b) elaborates

the reflection of EM wave due to output interface in thin film material for EMI shielding. Figure 4(c) explains the phenomenon of reflection due input interface of a material. Figure 4(d-g) explains the multiple internal reflection of porous, hollow, shell and solid material.

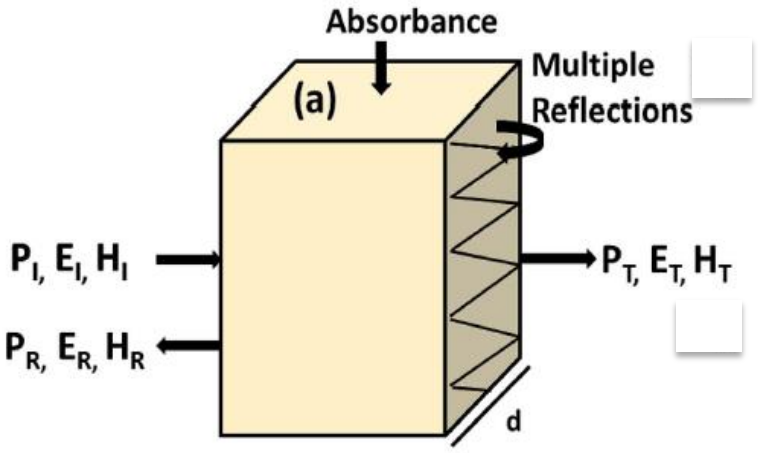


**Figure 4 (a)**

**Reflection, Absorption, Multiple reflection in 3D Material**

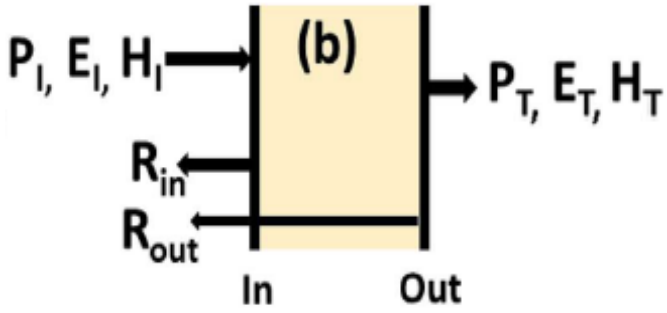


**Figure 4(b)**

**Output Interface as source of reflection for thin films**

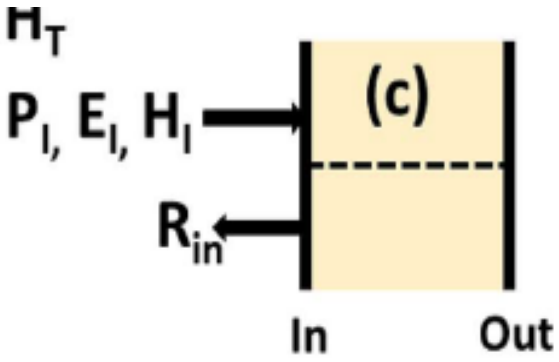


**Figure 4(c)**

**Input Interface as source of reflection of thin films**

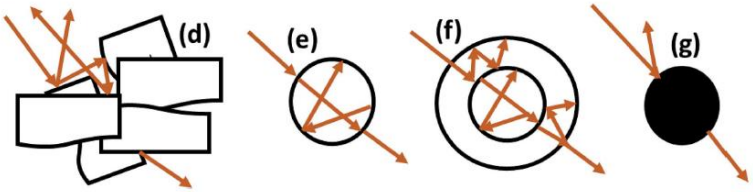


**Figure 4 (d-g)**

**Figure 4: Multiple reflections through various geometries**

## 1.5. Shielding effectiveness of material

Shielding effectiveness (SE) is represented as cumulative sum of all the losses i.e. reflection loss, absorption loss and multiple reflection loss in equation form as:

$$SE(T) = SE(R) + SE(A) + SE(M) \quad (Eq\ 7)$$

$$SE(T) = 10\log\left(\frac{Pi}{Pt}\right) = 20\log\left(\frac{Ei}{Et}\right) = 20\log\left(\frac{Hi}{Ht}\right) \quad (Eq\ 8)$$

Where:

| | |
|---|---|
| P: | Power |
| E: | Electric field |
| H: | Magnetic field |
| I: | Incident wave |
| R: | Reflected wave |
| T: | Transmitted wave |
| SE(R): | Net reflection |
| SE(A): | Net absorption |

SE(M): Net Multiple reflection

It is important to emphasize that secondary reflection shown in 3D material as well as thin films from output interface occurs only in finite dimensions materials, further effect of multiple reflection in thicker slab can be neglected and Equation 7 will be modified for thicker materials as:

$$SE(T) = SE(R) + SE(A) \qquad (Eq\ 9)$$

## 1.6. Primary factors contributing in Electromagnetic Interference Shielding

### 1.6.1. Reflection loss

The reflection loss occurs primarily due to impedance mismatching between the input interface and output interface of a shielding material and its magnitude is represented in equation form as:

$$SE(R) = 20\log\left(\frac{Zo}{4Zin}\right) = 39.5 + 10\log\left(\frac{\delta}{2f\Pi\mu}\right) \propto \frac{\delta}{\mu} \qquad (Eq\ 10)$$

Where:

δ: Conductivity

f: Frequency

μ: Relative permeability

Further, it can be noted that reflection loss has direct relation with conductivity (δ) and inverse relation with permeability (μ) of a shielding material. This implies that a shielding material requires mobile charge carriers (Electron or holes) for enhancing reflection properties of a material for incident EM wave. Thus, if a shielding material do not possess mobile charge carriers i.e. Electron or holes, this makes the conductivity (δ) constant and if the frequency of incident EM wave increases on a material with constant conductivity and permeability, the reflection loss SE(R) will decrease.

### 1.6.2. Absorption loss

2nd significant factor of EMI shielding material is the loss of intensity of EM wave due to absorption phenomenon. Plane wave theory describes the exponential amplitude attenuation of EM wave inside a shielding material that means absorption loss SE(A) occurs due to ohmic losses and induced current in any material.SE(A) losses in decibel can be represented as:

$$SE(A) = 20log\ e^{d/\delta} = 8.7d\sqrt{\Pi\delta\mu} \propto d\delta\mu \propto \alpha d \qquad (Eq\ 11)$$

Where:

d: Thickness of material

**α**: Attenuation constant

SE(A) mainly depends on conductivity (δ), permeability(μ) and sample thickness(d).Therefore, for conductive metals absorption is the dominating factor for EMI shielding rather than reflection. Moreover, the attenuation constant describe the reduced intensity of EM wave while passing through a material and represented by an equation as:

$$\alpha = \frac{4\pi n}{\lambda o} \qquad (Eq\ 12)$$

Where:

λo: Wavelength in vacuum

n: Refractive index given as $(\varepsilon\mu)^{1/2}$

In nonmagnetic material μ=1 so:

$$\alpha = \frac{4\pi\varepsilon^{\frac{1}{2}}}{\lambda o} \qquad (Eq\ 13)$$

It is clear that high permittivity of material is crucial for enhancement of SE(A) as well as SE(R).

### 1.6.3. Multiple Reflection loss

Shielding effectiveness due to multiple reflection like absorption loss mainly depends on the thickness of EMI shielding material. Multiple reflection phenomenon is more prominent in porous, hollow, shell or solid structure with irregular morphology. The irregularity, large area and voids gives more scattering, diversion to incident EM waves, hence enhancement in overall shielding effectiveness of material.

Up-till now we have been focusing on the shielding materials that have either reflective, absorbents or multiple reflective properties. However, practical scenario needs the tradeoff between fabrication of purely reflective, absorbent and multiple reflective materials b/c of other characteristics like weight, thickness, flexibility and strength of shielding material. Hence, instead of homogeneous material alone, composite materials with micro and Nano fillers of metallic and ferromagnetic particles is of vital importance for achieving better polarization and permeability for enhancing reflective and absorbing properties respectively. In composite materials permittivity and permeability both are complex, having both real and imaginary parts and are stated as effective permittivity and effective permeability respectively and expressed as:

$$\mathcal{E} = \mathcal{E}' + i\mathcal{E}'' \quad (Eq\ 14)$$

Where:

$i$: Imaginary number

Ɛ: Complex number

Ɛ': Electric energy storage capability

Ɛ'': Di electric loss

Similarly permittivity is given as:

$$\mu = \mu' + j\mu'' \quad (Eq\ 15)$$

Where:

j: Imaginary number

$\mu'$: Magnetic energy storage capability

$\mu$'': Magnetic loss

Complex permittivity and permeability having real and imaginary part needs the adjustment to certain value for effective reduction of reflection phenomenon for military application. Reduction of reflection phenomenon is possible only by decreases impedance mismatching between the free space and shielding materials. Transmission line theory explain the intrinsic surface impedance of composite material in term of permittivity and permeability as:

$$Zin = \frac{E}{H} = \frac{\sqrt{fj2\pi\mu}}{\sqrt{\delta + fj2\varepsilon}} \qquad (Eq\ 16)$$

The microwave absorption properties in term of reflection loss for EMI shielding material can be estimated by:

$$Rl(db) = \frac{Zin - Zo}{Zin + Z0} \quad (Eq\ 17)$$

Above equation tell us that minimum reflection loss and maximum absorption in EMI shielding material occurs only if the input impedance of material (Zin) matches with the impedance of air ($Z_0$). This implies that both Zin=$Z_0$ = 377Ω and this condition happens only on specific thickness (tm) and resonance / matching frequency (fm). The relation of specific thickness(tm) and matching frequency (fm) can be related in equation form as:

$$tm = nc/4fm\sqrt{\in \mu} \qquad (Eq\ 18)$$

Best way to minimize the impedance mismatching and increasing the absorption properties of EMI shielding material requires increase in effective permeability and decrease in effective

permittivity. The absorption phenomenon for EMI shielding material is more suitable in military applications because it reduces radar cross section by reducing reflection of incident EM wave, to provide military equipment with necessary stealth capability required for avoid detection and keep an element of surprise. Moreover, when an incident EM wave strikes an EMI shielding material with absorbing characteristic, the incident EM energy is converted into thermal energy through di electric or magnetic losses.

Till the time we are emphasizing 03 x phenomenon responsible for EMI shielding i.e. reflection loss, absorption loss and multiple reflection loss. Further, it was explained that relative permittivity and permeability of any material leads the reflection loss or absorption loss respectively. For electrical shielding the conductivity and polarization are the main contributing factors whereas for magnetic shielding ferromagnetic resonance, exchange resonance and eddy current are of prime importance. Besides all of above, size, morphology of shielding surface, time and temperature variations, and thickness of material and mass ratio of fillers in a material also play significant part in EMI shielding effectiveness.

## 1.7. Secondary contributing factors for EMI shielding

### 1.7.1. Size of fillers

Permeability is greatly affected by size and dimensions of filler particles. Eddy current losses responsible for thermal loss in a material decreases if the size of particle decreases below a critical size of filler because it decrease in critical size of filler decreases the induced Eddy voltage i.e Eddy voltage $\propto$ Area. Anisotropic behavior of structure (properties of substance to exhibit variation in physical properties along the molecular axis) dominates the Nano structure being of small size and breakage of some exchange bonds. This change in property modifies the spin relaxation time or frequency and it is believed that permeability is governed by relaxed state of time or frequency than intrinsic resonance in relaxation state of Nano structures. Spin fluctuations remain very fast b/c of smaller size in super paramagnetic state, further relaxation occurs at higher frequencies [15],[16-20].

### 1.7.2. Shape and morphology of particles/fillers

Polarization necessary for dielectric losses in EMI shielding material can be enhanced by fabricating complicated structures. These complicated structures basically enhance the Maxwell Wagner effect i.e. Charge separation over considerable distance in a heterogeneous material at interface by keeping different dielectric constant and electrical conductivity. This effect is

introduced in EMI shielding material by introduction of multi interfaces at the EMI shielding surface by keeping large surface area and high porosities. Further, unsaturated bond for dipole polarization in complicated geometries along with multiple interfaces is beneficial in EMI attenuation due dipole orientation and conductivity losses. Fe-Fe Alloy materials for EMI shielding observe the magnetic anisotropy and relaxation process [21].

### 1.7.3. Time and temperature variation

Structural changes occur inside any shielding material with variation of time and temperature. Increase in temperature increases disorder and create defects in the form of voids, introduction of immobilized free radicals or substitution of materials. It has been noted that reflection loss is reversed at certain temperature and creates an extra energy level around solid body by addition of an electron and hence enhance attenuation rather than reflection [22]. Further, reflection loss is also influenced by reaction time and temperature [23] in composite materials.

### 1.7.4. Mass Ratio

Percolation threshold (Mathematical concept defining the formation of long range connectivity of random system) governs the mass ratio for fillers to enhance electrical conductivity. This concept of percolation threshold can be represented in the form as:

$$\delta = \delta o(V - Vc)^c \quad (Eq\ 19)$$

Where:

- δ: Electrical conductivity
- δo: Conductivity of free space
- V: Volume content of fillers
- Vc: Volume content at percolation threshold
- C: Critical exponent

Percolation threshold is responsible for conductive networks within a matrix due to concentration distribution and compatibility of fillers for the matrix and its dependence lies on morphology, shape and conductivity of fillers as well [24].It has been noted that properties of composite materials start decreasing above the percolation threshold b/c mass ration generates dielectric relaxation and enhance eddy current effect by increase in eddy voltage within material responsible for magnetic loss [25].

### 1.7.5. Thickness of material

Thin material exhibits better multiple reflection phenomenon for EMI shielding effectiveness. However, increase in thickness brings variation in reflection peak shift towards lower frequencies. Coating either metallic by electroless plating, electrodeposition and magnetron sputtering also changes the microwave absorption properties of a material b/c EM wave dimensional resonance increases with increase of coating thickness. Critical thickness exhibits superior dielectric behavior for EMI shielding.

## 1.8. Objective of Research

To develop an EMI shielding material having good adhesion with Missiles body i.e. Aluminum Alloy and Mild steel.

## 1.9. Outline of the Thesis

**1st Chapter** Details the introduction of EM waves and their propagation within different interfaces of materials. Further, EMI shielding mechanisms, primary and secondary losses responsible for attenuation of incident EM wave and interaction of EM wave with different geometries and shapes of shielding materials is also discussed in detail.

**2nd Chapter** includes examples of the research work carried out to enhance the EMI shielding phenomenon by use of different polymers, metallic and ferromagnetic fillers and by addition of Nano particles.

**3rd Chapter** summarizes the experimental techniques and materials for synthesis of EMI shielding materials and various characterization techniques used to examine morphology physical and chemical properties of fabricated samples.

**4th Chapter** highlights the results obtained from different characterization techniques for all the synthesized samples, and elaborate the significance of results obtained for EMI shielding of Missiles.

**5th Chapter** concludes the entire work.

**6th Chapter** provides the future recommendations**.**

# Chapter 2
# Literature Review

The EM wave possesses potential threat for aircraft's electronics and even for the safety state of explosives during storage, transportation and use [26], [27]. To investigate safety related issues in Missile, Underwater weapons and military equipment, extensive literature review was carried out for exploring a material, that possess appropriate thickness, better adhesion, superior thermal and physical properties. To serve the ibid purpose, we scrutinized literature to identify a material that exhibit better adhesion characteristic with both Aluminum and steel along with possessing significant EMI shielding characteristics. For clear and concise picture and reaching a better conclusion, work spanning over the period of last two decades was studied in detail and brief summary extracted from literature to efficiently undertake our research. It was found in early 21$^{st}$ century; D.D Chung uses carbon material for EMI shielding using electroplating technique for EMI shielding. He selected nickel as a metal considering better properties for coating in electroplating process. Further, he emphasized on use of small size particles for better use of entire cross section in EMI shielding applications. He also explained that filaments of carbon and nickel both showed better EMI attenuation than particles, of course the Nickel filament depict highest EMI attenuation due to superior oxidation resistance than silver and carbon filaments [28].Pavel Steffan et.al work was focused on EMI shielding of concrete structures. His work mainly highlighted the use of Short carbon fibers (SCF) and chemical agents for enhancing EMI shielding of cement mortar. He explained that inclusion of SCF and chemical agents not only enhance EMI shielding significantly but also improved flexural and tensile strength of concrete structures. Inclusion of 0.5% weight of SCFs in total weight of cement enhanced EMI shield up to 10dB in 4mm thick cement mortar and clearly indicated that shielding effectiveness attained by this method is considered enough for EMI proofing of structures [29]. Xiaohu Hung et.al uses electroless or autocatalytic plating method for Nickel Cobalt coating on bi-carbon Nano fiber web. Electrical conductivities of fabricated material was investigated by four probe method and

vector network analyzer (VNA) is used to measure for EMI shielding. Scientist explained that Nickel Cobalt depicts better electrical, mechanical and anti-oxidant properties, which leads to EMI attenuation of 41.2dB in NCCF with 30% weight of paraffin wax used for hardening of composite material [30]. Fawad tariq of SUPARCO Pakistan fabricated a light weight EMI shielding material by use of Carbon fibers (CFs) and Multiwall Carbon Nano tubes (MWCNTs). These hybrid Nano composite materials showed better electrical properties for EMI attenuation. This work highlighted that addition of .25% weight of MWCNTs in CFs enhanced shielding effectiveness (SE) in frequency ranges 1-8 GHz. Higher concentration of MWCNTs gives better shielding effectiveness for higher frequency ranges than 10GHz [31].

In late 2015, J Ziaja uses two source magnetron sputtering with titanium (purity 99%) and brass alloy with diameter target of 50mm in argon atmosphere with group frequency (fg) 50Hz-5KHz and time applying frequency of 5mins on each side of material. Brass Alloy showed better EMI attenuation than titanium. Addition of titanium less than 20% weight exhibits no effect of shielding effectiveness of material, hence using magnetron sputtering techniques shielding effective up to 40dB can be achieved at faster rate [32]. Ionut balan, Cristan Morari and Alexandru Eros patroi investigated the effect of Ni and Fe fillers in silicon rubber carbon mesh. Experimental setup for far field condition using two horn antennas in anechoic chamber using VNA was established for EMI shielding measurement. He explained that carbon mesh being conducting in nature is the main contributory factor in attenuation of EM wave in frequency range of 0.9-4 GHz [33]. Young Seok byune et al introduces a new measurement technique for EMI Shielding measurement i.e. Nuclear Magnetic Resonance (NMR). NMR can be used efficiently for small flexible composite materials. He used Hanji (Korean paper) doped in Carbon Nano tubes (CNTs) exhibits better shielding than CNTs alone [34]. Kanthasamy Raaglulan et al fabricated Mxene oxidized CNTs based composite material with shielding effectiveness upto 50.55dB, further, the Mxene based composite possesses excellent thermal, electrical properties [35].

In 2019, two novel techniques were used for fabrication of EMI shielding material i.e coagulation method and vacuum deposition. Both these techniques were never being applied for fabrication of EMI Shielding materials. Vidhya et al fabricated EMI shielding material based on coagulation process, he used Carbon black (CB) for conduction and strontium yttrium cobalt oxide (SYCO) as a ferromagnetic material at room temperature in Poly Vinylidene Fluoride

(PVDF). This article explains that all three contributing factors for EMI attenuation i.e. Reflection loss, Absorption loss and multiple reflection loss are considerably enhanced by addition of CB, SYCO filler in PVDF and hence attenuation up to 50.2 dB of EMI wave in composite material was observed [36]. Avi bregman uses vacuum deposition for EMI shielding of composite material. He introduced pores in composite material made of Nano Graphene platelets (X GNP) and poly lactic acid (PLA) and explained that even distribution and shape of pores effect EM wave attenuation. His work explained that spherical shaped pores increases shielding effectiveness up to 13dB in a material fabricated by vacuum deposition technique. Further, he introduced the concept of perfect electrical conductor (PEC) backed composite material that can be used to decrease fraction of reflected power and increase absorbing characteristics of composite material for EMI shielding. His idea of pore adjustment brings novelty in EMI shielding of material by changing pores orientation and shape [37].

## 2.1. EMI Shielding processes

### 2.1.1. Metal sheet

Metal sheets are thin flat pieces formed via various forming processes i.e. press brake forming, punching, roll forming, rolling, spinning, stamping, water jet cutting and wheeling etc. Sheet metals are divided in different categories based on their thickness for e.g. thin sheets are considered as foil or leaf and pieces thicker than 6mm are considered as plates. Sheet metals are available in various forms and shape i.e. flat pieces or coiled strips depending on nature of application. Usually metal sheets thickness ranges in mm and unit of measurement is called Gauge. Gauge differs with nature of material whether ferrous (Iron based) or non- ferrous (metal). Metals used in sheets are brass, copper, steel, nickel, tin, titanium or aluminum. Metal sheet possess higher permeability (Magnetic property) and hence a valuable contenders of EMI applications but main drawback is huge weights.

### 2.1.2. Electroless deposition

Electroless deposition (ED) or chemical bath deposition (CBD) refers to redox reaction for deposition of thin film on conductive or insulating base material. Material such as zinc, lead, cadmium has been used for formation of thin films in various applications. Similarly, metals like nickel that possess higher ferromagnetic behaviour can also be used for thin film coating on polymers or conducting substrates for EMI shielding behavior [38]. Chemical bath deposition (CBD) or Electroless deposition (ED) work on principle of redox reaction (Chemical reaction for

transfer of electrons for changing oxidation state of atoms, in redox reaction one chemical specie undergo oxidation and other specie undergoes reduction). ED show slow release of anions with free metal ions in a solution. Hence, thin film is formed on substrate due to ion-by-ion deposition and this ion-by-ion growth leads to mirror like film. Schematic diagram of Electroless deposition is shown below.

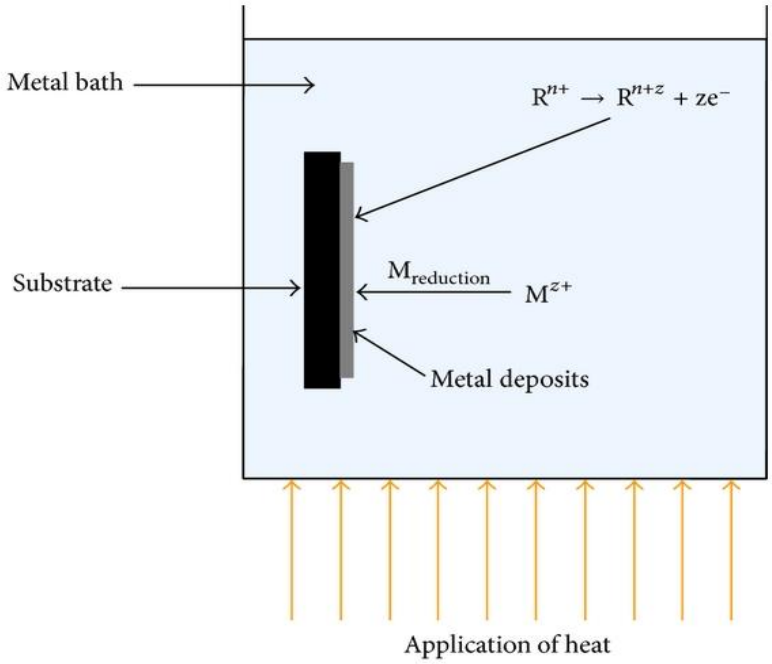


**Figure 5: Electro-less Deposition**

### 2.1.3. Electro plating

This process is generally used to change the surface properties of material but it can also be implemented to change chemical properties of substrate. In this process electrical potential is applied on both electrodes i.e. cathode and anode for reducing dissolved metal cations that can lead to formation of thin coherent coating. It is also called oxidation of anion on solid substrate. Hence, this method can also be used for EMI coating. Electro plating can be done by various methods like electro chemical deposition, pulse electroplating and brush electroplating for localized area of material.

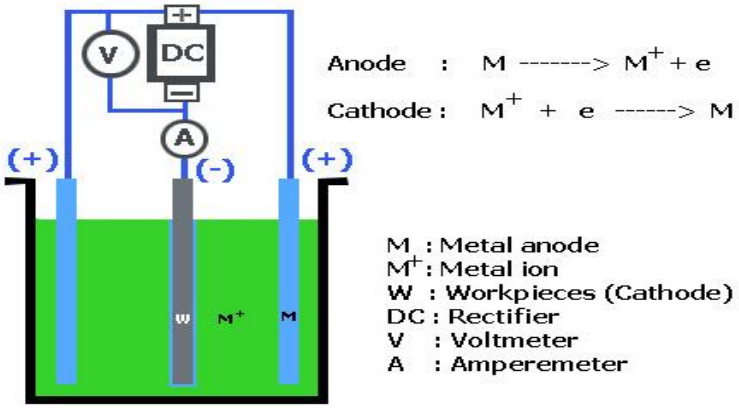


**Figure 6: Electroplating**

### 2.1.4. Magnetron Sputtering

Magnetron sputtering works on principle of physical vapor deposition for fabrication of thin films. Magnetron sputtering has large applications in thin film fabrication due to its benefit of purity and cost effectiveness. The process works on ejection of electron / particles from source called target and substrate is placed at upper surface for coating. It is actually collision process between the incident particle and target. High speed sputtering needs increase in ionization rate of gas to reduce pressure in closed environment. The incident particles / electron undergo complex scattering hence momentum shift of atoms occurs as it is a cascade process in which one atom shifts it momentum to striking atom and hence this momentum moves to final atom which will collide the surface of substrate with maximum force. Variation in electric and magnetic field is maintained to make particle to follow the trajectory and increases probability of hitting of ejected particles to surface of substrate needs to be coated [39].

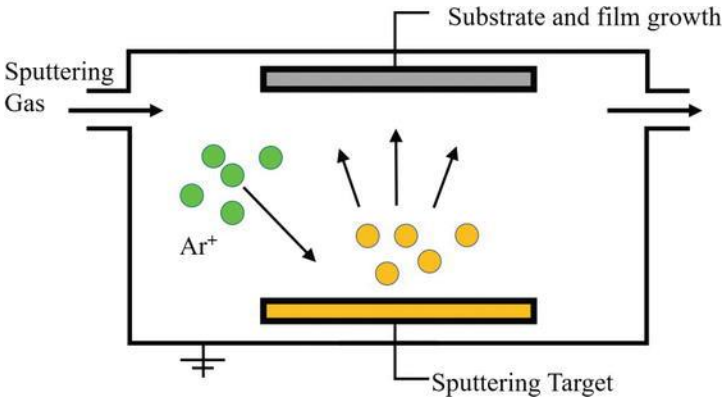


**Figure 7: Magnetron Sputtering**

### 2.1.5. Polymer based EMI shielding materials

Polymer based EMI shielding materials are widely in use due to their light weight nature. Wide variety of conducting as well as insulting polymers is available for fabrication of EMI shielding materials. Conducting polymers have advantage over insulating materials for EMI shielding as they can be used with and without fillers for EMI shielding but these polymers are expensive. However, insulating polymers needs conductive fillers for attenuation of EM waves. These polymers are to be dissolved in solvent and for composite preparation it is necessary that both the fillers and polymer are soluble in same solvent to reduce impurities effect in fabrication of final form of composite material. Composite materials can be fabricated in various ways via solution casting, coagulation process and vacuum deposition. However, before selecting any process homogeneous mixing of polymers in solvent is the key factor to be taken care of. Therefore, complete analysis of various homogeneous mixing techniques need to reviewed prior selecting process of fabrication.

## 2.2. Composite preparation processes

The main concern in composite preparation is the mixing process. Composite materials for EMI shielding are obtained by homogeneous mixing of Nano particles and Nano sheet in polymer. Therefore, prior to the composite preparation, the compatibility between the two components has to be assured to avoid agglomeration. The methods for preparation of composite material after homogenous mixing of the polymer composites are explained below.

### 2.2.1. Melt Blending

Melt blending is normally used method in composite preparation due to its efficiency and operability. In the process, the polymer and the inorganic filler (i.e., silica) are sheared in the melt at a temperature which is equal or more than the melting point of the composite. Under suitable conditions the material exfoliates and disperses to some extent. This technology is very versatile and can be applied to various polymers. It is also possible to add swelling and capitalizing agents in order to improve the exfoliation and reach a better adhesion between the two major components. Solution blending, on the other hand, is a liquid phase powder processing process that allows excellent molecular mixing. Solution blending can be achieved by either dissolving only the polymer matrix or dissolving both the matrix and the nanoparticles.

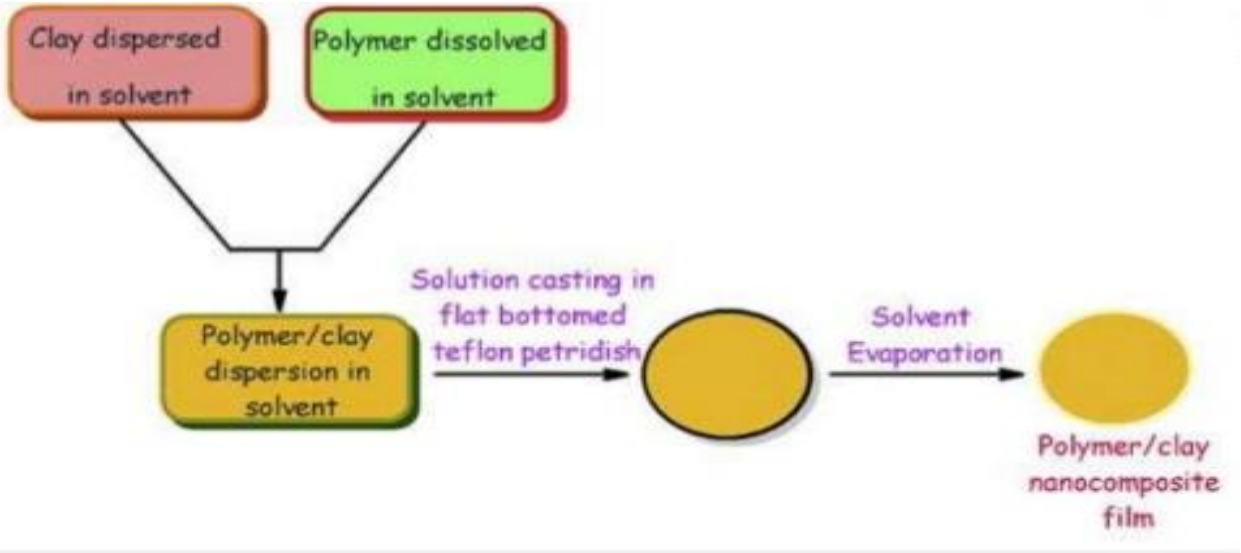


**Figure 8: Melt Blending**

### 2.2.2. Sol-gel process

The sol-Gel method is a synthesis which contains production of a sol, the effective gelation and the solvent removal. In the history sol-gel process is usually used to synthesize novel organic polymer composites or inorganic polymer Nano-composite. In the field of composites, the aim is to carry out the Sol Gel reaction in the presence of polymer molecules have various functional groups that enhance their bonding to the inorganic section.it proves to be an affective increasing strength method that can increase filler particles within a polymer matrix.

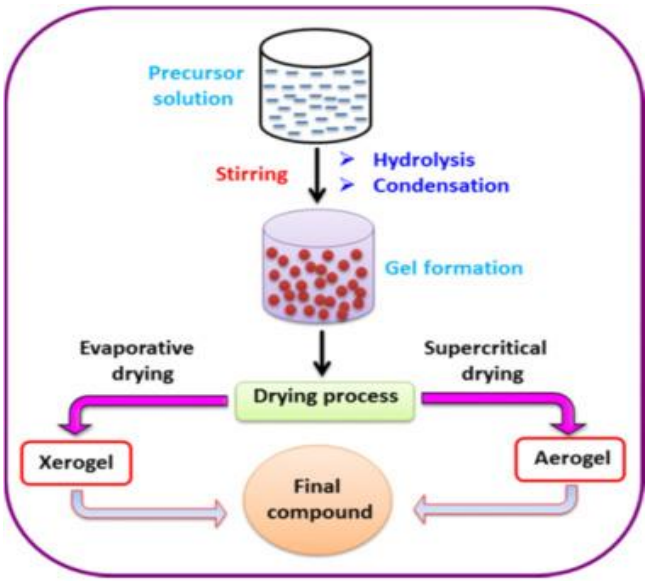


**Figure 9: Sol Gel Process**

### 2.2.3. In situ polymerization

In situ polymerization is a very successful and fast way to build a Nano-composite. In this process, the inorganic fillers have initial treatment with specific surface modification elements and then mixed directly to the liquid resin during the polymerization. With the help of solution method, Nano particles are introduced to a composite solution by the help of solvents such as THF, chloroform and acetonitrile to integrate the polymer composite and Nano particles.

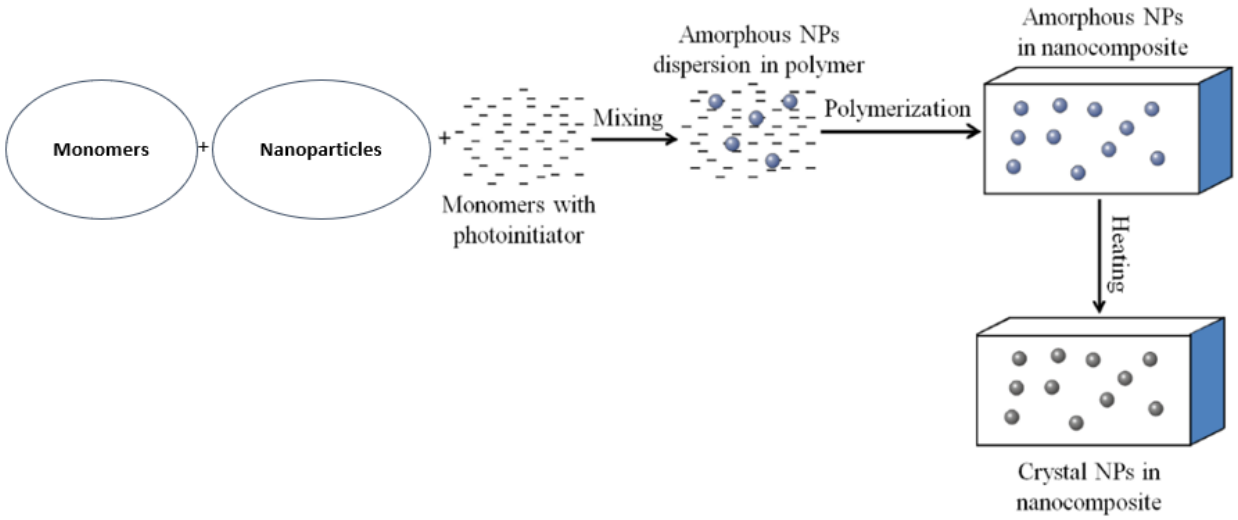


**Figure 10: In Situ Polymerization**

### 2.2.4. Resin film infusion process (RFI)

The Fabric is sandwiched between epoxy resin films. This sandwich of the resin film and fabric is then placed atop of a mold plate made of metal. The reason for doing this is to assure that the fabric will absorb the film. This sandwich of resin film and fabric is then cut according to our requirements. These slivers are placed atop of each other to get the thickness required. Vacuum is applied and measured, using a sensor, to the resin film and fabric sandwich. This can be done in a convection oven by vacuum bag method. This is done for the curing of the resin film and fabric sandwich. Then the sandwich is heated to a maximum temperature of 80°C at a heating rate of 2°C and this temperature is held for 30 minutes. The specimen is then heated at 120°C for 60 minutes. This is done to cure the specimen. After this the heating is turned off and we allow the specimen to cool. It is cooled down to 25°C slowly. Then it is demolded [40]. Synthesis of

various hybrid composites is possible at different concentrations. Compared to respective control composite specimens, their characteristics have been appraised.

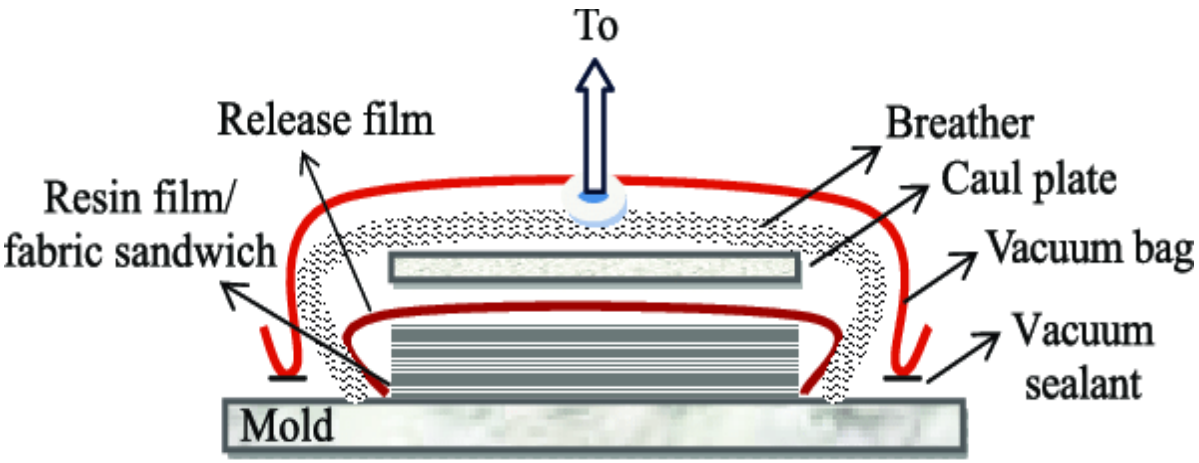


**Figure 11: Resin Film Infusion Process**

### 2.2.5. Solution cast process

Solution casting is the process for composite formation through thermoplastic materials. This is three way process starting from stirring via magnetic stirrer of polymer in a soluble solvent, 2nd step is casting of solution on a glass or material with whom polymer does not possess adhesion and third process involve drying of solution at certain temperature to form a composite material for subsequent use. The steps involved in whole process of solution casting are illustrated via diagram.


**Figure 12: Solution casting**

## 2.3. Conclusion

Through a comprehensive literature review of the techniques and study of current trends for Electromagnetic Interference Shielding across the globe, melt processing was deduced to be the most common procedure for polymer nanocomposite development and Magnetron Sputtering coating technique was considered to be fastest process for EMI shielding. However, both these techniques are very expensive. Therefore, solution casting technique for synthesis and polymer based material was tried being novel in the field of EMI shielding and financially attractive option. Solution casting process is preferable for specific composite structures. Materials synthesized by solution cast process are time efficient to other EMI techniques. Materials manufactured by solution cast process have brilliant drapability along with better dispersion for Nano particles and Nano Sheets. Solution cast method additionally guarantees the substantial reduction in capital cost. In addition, for large scale production, this is the main procedure that encourages fabrication of composites with consistently scattered Nano materials. Next chapter describes in detail the materials and experimental methods being applied for fabrication of EMI shielding material.

# Chapter 3

# Materials & Methods

## 3.1. Materials Used

Industrial grade PET Poly(ethyleneterephthalate) with intrinsic viscosity of (0.81 dL/g) was provided by ECOPACK LTD. N-methyl-2-Pyrrolidone (NMP) was purchased from Sigma Aldrich and Hexagonal Boron Nitride was purchased from local vendor.Aluminum Alloy and Stainless steel Military standards were requested through Strategic Organizations.

## 3.2. Nano sheets Synthesis

3g of hexagonal boron nitride powder mixed with 60mL of NMP in a 70mL capacity metallic cylinder was sonicated for 48hrs using a 120 hertz fixed frequency sonicator at 60 amplitude with a 2 sec ON and 1 sec OFF pulse in a cooled water bath. Resultant solution contained exfoliated Nano sheets of varying aspect ratio, centrifugation at 1500rpm was applied for their separation, supernatant obtained in centrifuge tubes was collected and vacuum filtered on a PET membrane of 0.4um pore size to get rid of the excess NMP, filtrate containing membrane was then placed inside oven at $60^{o}$C overnight to obtain the desired Nano sheets, same procedure was then repeated at 700 and 500rpms. Nano sheets were characterized using XRD. (**Figure 13**) further illustrates the process.

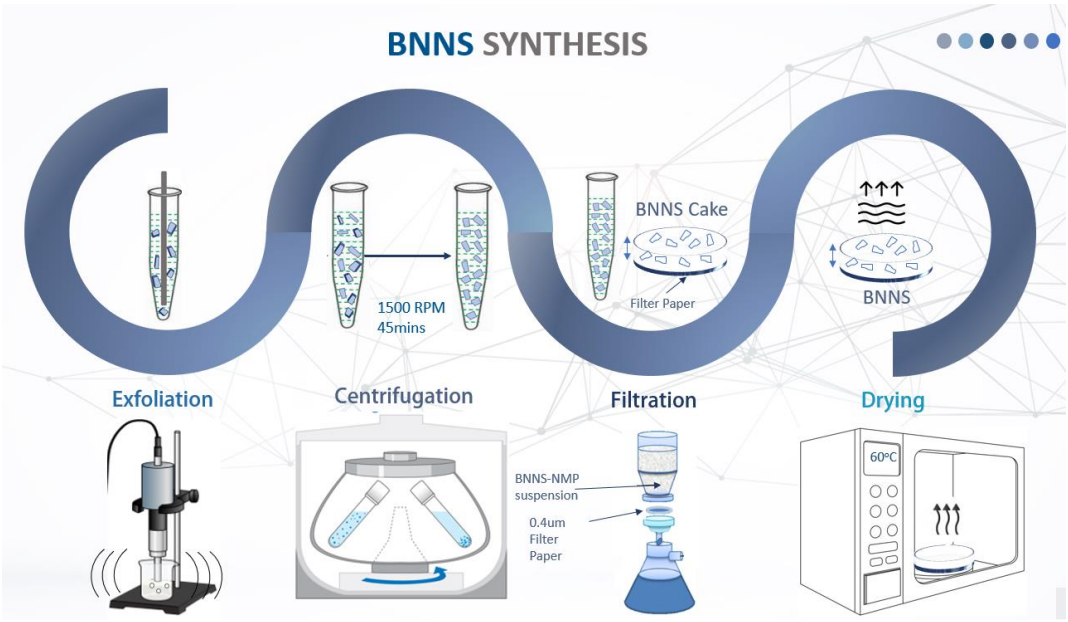


**Figure 13: Boron Nitride Nano sheets Synthesis**

## 3.3. Nanocomposite film Synthesis

All composites were fabricated using 1500rpm BNNS. PET membranes, pure and Nanocomposites were synthesized using TIPS. PET pellets were dissolved in NMP at a temperature higher than its $T_g$ (>165$^oC$) with constant magnetic stirring (200rpm) inside a 20ml black cap glass vial. Solution concentration was set at 550mg/10mL. Pellets were seen to be completely dissolved in 15-20 mins, Nano sheets of desired concentration were then added and solution was further stirred magnetically on hot plate for further 15-20 mins to ensure uniform dispersion of Nano sheets inside polymer matrix, however, the color of solution was seen to shift from transparent to dark yellow brownish with time. Polymer chain disassociation and acetaldehyde formation while heating could be the possible reason for this occurrence [41]. Afterwards, solution was casted with great care in a 3 inch glass petri dish placed in oven at elevated temperature. Thin films were formed as soon as the solvent had evaporated. Thin films were seen to be extremely sensitive to evaporation time and evaporation temperature. (**Figure 14**) further illustrates the as described process.

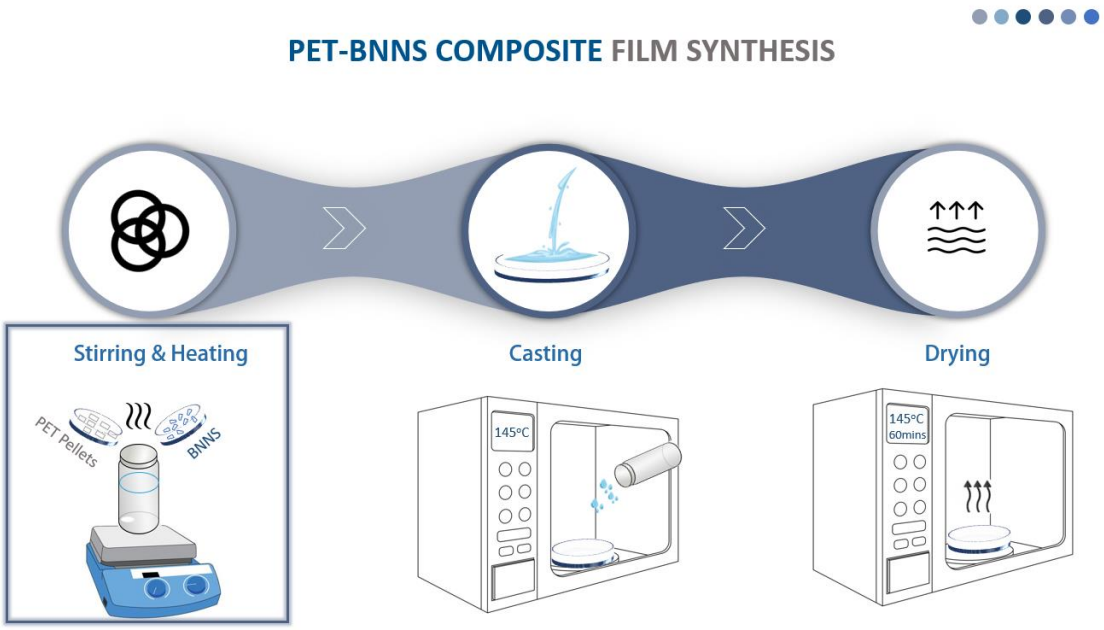


**Figure 14: PET-BNNS Nanocomposite Synthesis**

## 3.4. Optimization of Parameters for PET film synthesis

### 3.4.1. Evaporation Temperature

Temperature optimization for PET film synthesis could be divided into two sections: 1- Above glass crystallization temperature (**Tg**) and 2- Below (**Tg**). **Tg** for PET is 67$^{o}$C for amorphous and 81$^{o}$C for crystalline PET. PET polymer used for current research was semi-crystalline as observed and shown in XRD analysis, therefore its **Tg** lies somewhere between 67-81$^{o}$C. PET films formed below **Tg** were completely amorphous and fragile and not suitable for testing, they would break by slightest of contact with anything rigid. PET films formed above **Tg** in 100-130$^{o}$C range were brittle with enhanced strength than below **Tg** films but still unsuitable. Films formed in the region of 130-150$^{o}$C range depicted enhanced strength. As the temperature was enhanced further, strength of film increased but with increased brittleness. In addition, increase in temperature was also associated with an increase in density of films. 145$^{o}$C was chosen to be the ideal and optimized temperature for PET film synthesis where strength, ductility, brittleness and pore size were optimum for EMI Shielding phenomenon. Furthermore, with increase in temperature the appearance of films went from white (100-120)$^{o}$C range to brownish color in

(120-200)$^{o}$C range. All PET Nanocomposite films were prepared at 145$^{o}$C evaporation temperature.

### 3.4.2. Evaporation Time

After having fixed the variable of evaporation temperature, evaporation time was optimized. It was observed that optimum time for 145$^{o}$C was around (1hr-1hr5)mins, if heated for longer the film became too brittle to be tested and broke at the slightest of contacts. It was also observed that for every 10$^{o}$C rise in evaporation temperature resulted in a decrease in evaporation time by ~10mins.

### 3.4.3. Concentration of PET

PET films were synthesized with concentration of PET ranging from 300mg/mL to 550mg/mL. It was observed that PET films with concentration from 300mg/mL to 500mg/mL were too thin to be tested for EMI shielding effectiveness because of their fragile nature. All PET Nanocomposite films were then prepared with 550mg/mL concentration.

### 3.4.4. Effect of stirring RPM and stirring time

Preliminary PET film samples synthesis contained peculiar spots on the surface, these were assumed to be caused by the non-uniform dispersion of BNNS. To resolve the non-uniformity of PET film's surface first stirring time and its rpm for the dissolution step were varied. Stirring time was varied from 30mins to 1hr by keeping rpm fixed at 500 and it was observed that optimum stirring time for dissolution was 1hr since it reduced the non-uniformity to a great extent. Any further increase in stirring time would cause the PET, NMP, and BNNS mixture to turn brownish thereby adversely affecting the aesthetics. To further optimize the aesthetics of PET film surface, rpm was varied by keeping all other variables constant. Values were varied from (100-500) rpm, it was observed that at higher rpm values the dissolution time increased because at higher rpm values PET pellets would rise in a glass vial and were farther from the heating plate surface thereby taking longer to dissolve, whereas at 100rpm PET pellets were on the bottom of the glass vial and thus closer to the heating surface thereby taking fewer time to dissolve. Since rpm effects the stirring time therefore its indirect adverse effect was mitigated by keeping rpm value fixed at 100. Even after optimizing these two variables there still existed some non-uniformity on PET film's surface.

### 3.4.5. Effect of Probe Sonication

Sonication was applied after having fixed the rpm and stirring time variables to eliminate the non-uniformity patterns. Sonication amplitude and frequency was set constant at 60amp and 120hertz. Sonication was applied after PET dissolved (15-20) mins. Effect of sonication was observed by varying the sonication time and keeping all other variables fixed. Sonication time was varied from 1min to 1hr and it was observed that sonication did not have any effect on the dispersion of BNNS inside polymer matrix and the peculiar spots on the surface of PET film still existed.

### 3.4.6. Effect of Casting Position inside oven

Having observed no significant improvement in the optimization of aesthetics of film's surface, it was assumed that the issue persisted because of non-uniform heating and consequently evaporation of solvent. To mitigate this issue position of casting inside the ovens was optimized. PET films were casted at different positions in 3 different ovens. It was observed that position had a very significant impact on the aesthetics of film. All ovens had a different position where there was uniform heating and consequently uniform evaporation and these positions were not the center of the ovens. Optimizing this pattern removed all the spots that resulted due to uneven heating. Even after optimizing the casting positions there still existed some patterns on the surface of films

### 3.4.7. Effect of Lid of the glass vial

It was observed that all the non-uniform patterns disappeared in films that were casted with dissolution step performed without the lid of glass vial. The reason for this strange phenomenon is the fact that during the dissolution step, with the lid intact when the solvent evaporates it gets condensed on the inner surface of the lid due to temperature difference. The condensed solvent then falls back into the bulk mixture, therefore at any time during dissolution step there existed in the bulk NMP at lower temperature than the rest of the bulk temperature. When the lid was removed, and the mixture was casted on petri dish inside the oven the cooler NMP took longer time to evaporate than the rest of NMP thereby causing patterns on the surface. The issue of patterns was finally eliminated by removing the lid during the dissolution step. Table 2 contains the final optimized all variables.

**Table 2: Optimized Variables**

| Evaporation Temperature | Evaporation Time | Concentration | Stirring time | RPM | Sonication | Lid |
|---|---|---|---|---|---|---|
| 145$^{o}$C | 1hr | 550mg/Ml | 1hr | 100 | None | None |

## 3.5. Characterization

### 3.5.1. Working principle of SEM

The science behind the process of scanning electron microscopy (SEM) is the interaction of electrons with specimen material. When an electron beam is introduced into a column of the Scanning Electron Microscope, it does not encounter any atoms of any gas or liquid, in the atmosphere because a vacuum is established in that column. There is no interaction of electrons with matter, until it encounters the highly dense solid material. When the electron beam is incident on a sample, it transfers some of its energy to the molecules in the sample. This causes it to be reflected at an angle to its original well-defined trajectory. This results in the formation of back-scattered electrons, secondary electrons and X-rays. These interactions give us much needed information about the topography, composition, crystal structure and the presence of any electrical and magnetic fields. All these interactions result in the scattering of electrons, which can be classified into two main types, elastic and inelastic scattering, as shown in (**Figure 15**).

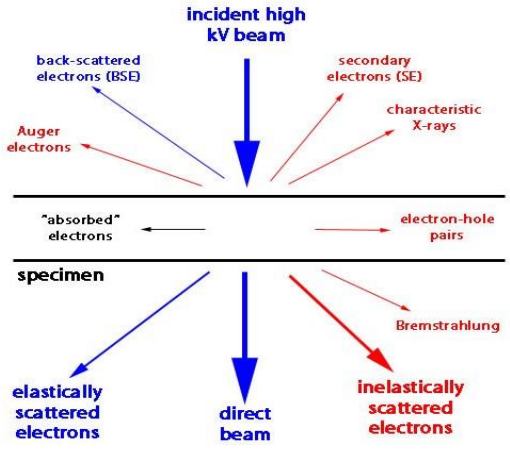


**Figure 15: Scattering of electrons on interaction with matter**

Scanning Electron Microscopy (SEM) is used to study the morphology of membranes. It can also be used to study the presence and distribution of pores throughout the membrane. For this purpose, electrons are produced by an electron gun, passed through accelerating voltage which causes them to travel quickly down a column, through many lenses and apertures, The lenses and apertures are used to produce a focused beam of electrons which ultimately hits the sample. The sample is placed in the chamber area. As the electrons are supposed to be focused onto the sample, therefore both the column and the sample chamber must be under vacuum, which can be brought about by a series of pumps. The beam is focused on to a particular area of the material by using scan coils, located directly above the objective lens. The scanning of the electron beam over that region of the sample helps us in studying the properties of a particular portion of the sample. Different signals are given out from this process which are then captured and analyzed by suitable detectors. The main components of the Scanning Electron Microscope (SEM) are:

- Electron source
- Column and electromagnetic lenses
- Electron detector
- Sample chamber
- Display screen

The schematics of the Scanning Electron Microscope can be shown as follows.

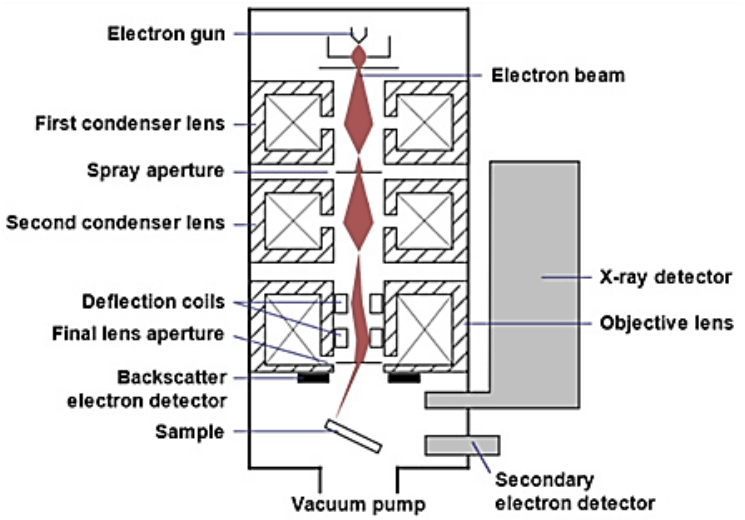


**Figure 16: Schematic diagram of Scanning Electron Microscope**

SEM analysis is performed by using TESCAN MAIA3 Field Emission Scanning Electron Microscopy (FESEM) for determining the morphological properties of the membrane samples. All the membrane samples having .005%, .010%, .015%, 0.25%, 0.050% and 0.075% w/w (filler-to-polymer) PET/BNNS films were characterized using this arrangement for the study of their pore distribution and pore structure. The analyses are performed at an accelerating voltage of 2 kV and magnifications of 5000x, 10,000x, 15,000x, 20,000x, 25,000x and 30,000x. The final SEM images were then studied to determine their surface features.

### 3.5.2 Working principle of Tensile Testing Machine

Tensile strength of a material is the maximum stress that a material can withstand until it breaks. There are different classes of materials, based on their mechanical strength. These include glassy and rubbery materials. The classfication into these two categories depends on their stress-strain behaviour. The glassy materials are rigid and brittle, whereas the rubbery materials are mostly flexible. The stress-strain behaviour of various types of materials is shown in (**Figure 17**)

In this figure, the curve shows that the brittle (glassy) materials show a high tensile strength, which is the end point of each curve here, but shows only small amount of strain. Whereas, the more flexible rubbery material shows a large strain, but a significantly lower tensile strength.

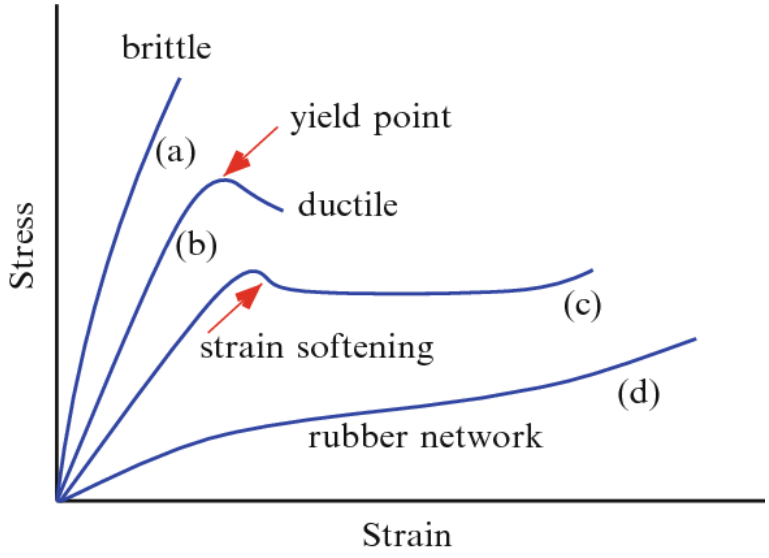


**Figure 17: Stress-strain behavior of several classes of materials**

.

The Tensile Testing Machine can be used to find out the tensile strength of the membrane materials. This machine consists mainly of a load which is connected to a movable upper jaw, to which one end of our test material is clamped. On the other end, is the fixed lower jaw which is held to the base, where the other end of the test material is clamped. When the material is safely held by the two jaws, the command is given from the computer connected to the machine, to start the test. This initiates the steady elongation of the material by the upward movement of the movable upper jaw. The movement is controlled by the elongation rate of the material, which is also known as the test speed as the elongation rate is dependent on the speed at which the upper jaw rises. The test automatically stops at the point where the material breaks. The schematic diagram of the tensile testing machine can be shown in (**Figure 18**).

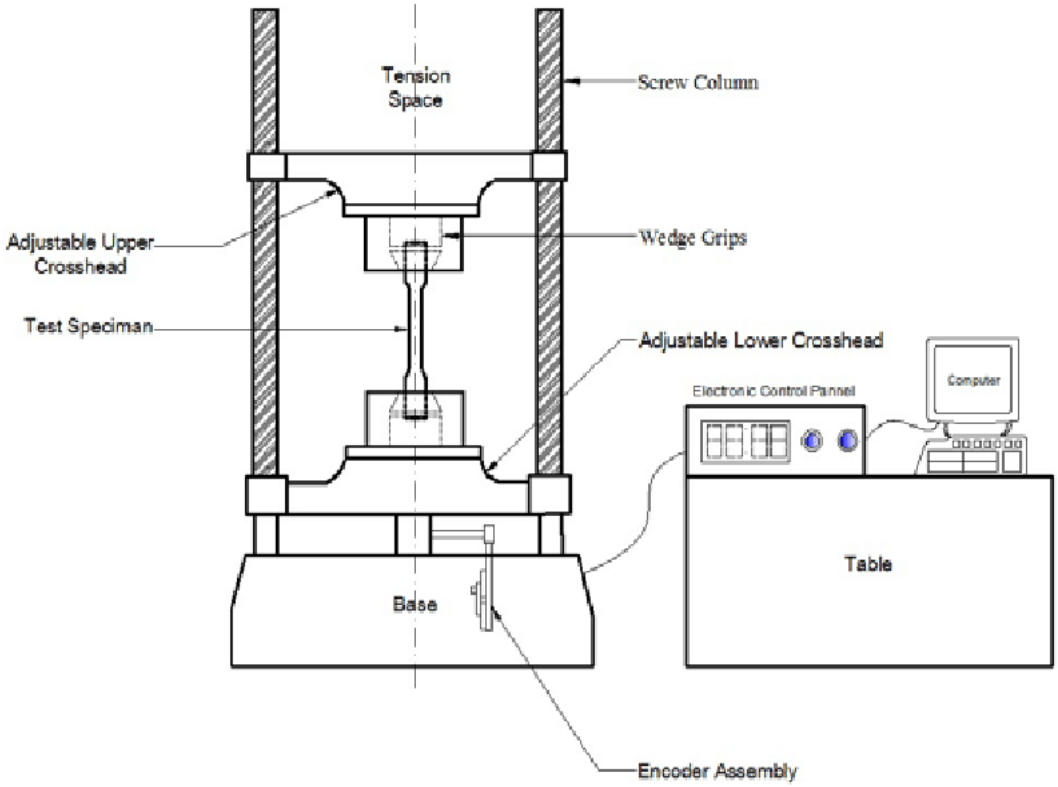


**Figure 18: Schematic diagram of Tensile Testing Machine.**

Tensile testing of all the samples i.e. 0.005%,0.010%,0.015%,0.025%, 0.050%, 0.075% PET/BNNS films was carried out, using SHIMADZU AGS-X series precision ultimate tensile tester with a full load of 20 kN. All the samples were tested using the ASTM standard D882-02, so the strips to be used were cut according to the dimensions provided by the standard. Finally, the stress-strain behavior was studied for the tests conducted using the said standard.

### 3.5.3. Working principle of FT-IR Spectroscopy

When infra-red radiation is incident on matter, it is absorbed by the matter. There are several vibrational states of a molecule. Once the radiation is absorbed, it causes the molecules to go from the ground state to the excited state, which means that the molecule goes to a higher vibrational state. The amount of energy needed to transfer the molecule to that higher state is proportional to the wavelength of the radiation absorbed. Every particular molecule has several functional groups in it, each of which absorbs radiation in a different specific wavelength, which is then called the *fingerprint* of that functional group. All the characteristic absorption peaks of each functional group combine to form the spectrum of that particular molecule, which is generated and studied using the FT-IR spectrometer.

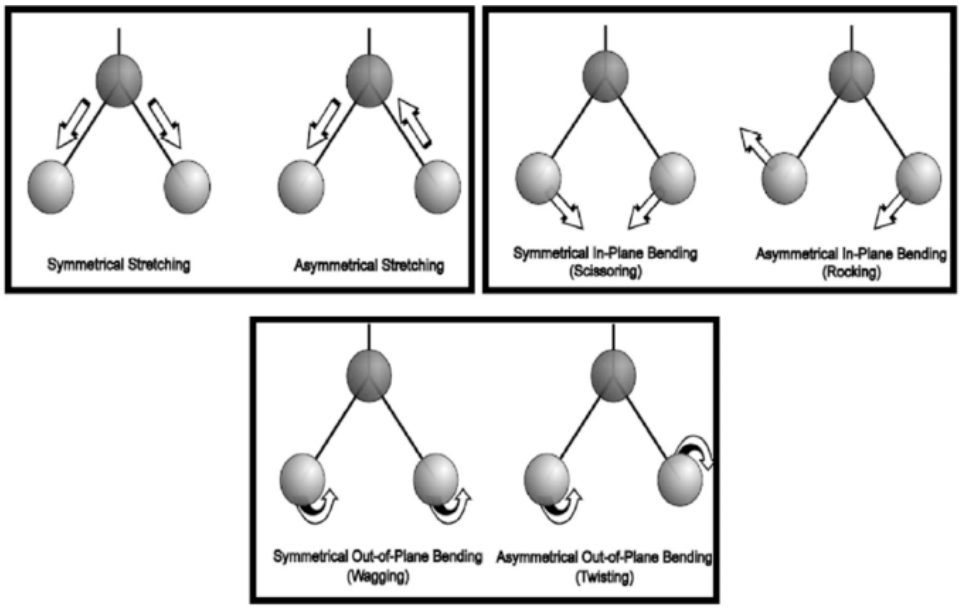


**Figure 19: Different modes of Stretching and Bending vibration**

FT-IR stands for Fourier Transform Infra-Red spectroscopy. It is a major analytical technique for the detection and determination of the identity of functional groups in a sample. When infra-red (IR) radiation is incident onto a sample, some radiation is absorbed by the sample, while some part of it passes through it. Whether we study the absorbance or transmittance of radiation, there is a certain characteristic spectrum, which results from a particular material. This is called the *fingerprint* of the sample. A FT-IR spectrometer consists of the following parts:

- IR source
- Beam splitter
- Fixed and movable mirrors
- Sample cell
- Detector

Inside an FT-IR spectrometer, an IR source generates infra-red radiation, which then is incident into a beam splitter. Here, the beam is split into two parts, one goes into the fixed mirror while the other goes into the movable mirror. This is done to take out only that portion of the IR spectrum, which is necessary for our analysis. The resulting beam is then recombined into one beam, and now contains only that region of IR which is required. This resulting beam then goes into the sample cell, where the absorbance of radiation takes place. Then, according to our requirements, the resulting spectrum is sent to the detector. The detector output is converted into interpretable spectra. FT-IR uses interferometry to record information about the material in the form of interferograms, and Fourier Transform is used to convert these interferograms into spectra which is used to identify and quantify the material.

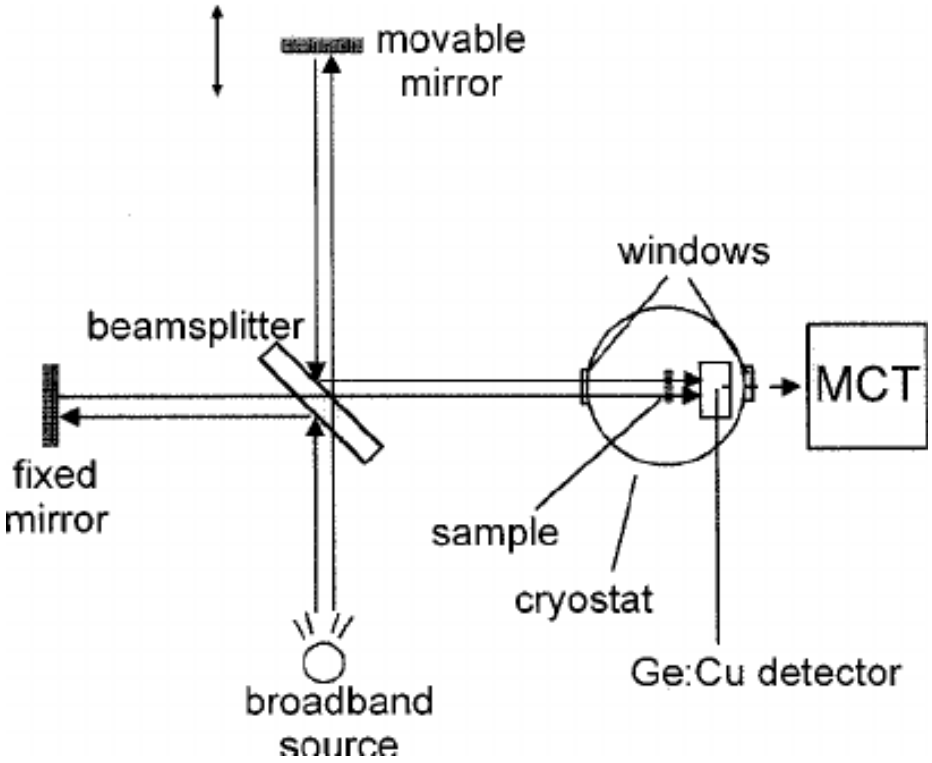


**Figure 20: Working principle of FT-IR spectroscopy**

FT-IR Spectroscopy was carried out using Perkin-Elmer Spectrum 100 FT-IR spectrometer. The analysis was carried out in the wave number range of 4000-400 $cm^{-1}$ and at a resolution of 4 $cm^{-1}$. The film samples were tested by cutting out a suitable sized sample and fitting it into the sample cell of the spectrometer. After fitting the membrane sample into the sample cell, IR radiation was then incident on the sample membrane. This resolve the film into its functional groups, which were .then studied when the spectrum is formed.

### 3.5.4. Working principle of AFM

An AFM uses a cantilever with a very sharp tip to scan a sample surface under investigation. As the tip approaches the surface, the attractive force between the surface and the tip cause the cantilever to deflect towards the surface. However, as the cantilever is brought further closer to the surface, such that the tip makes contact with it, increasingly repulsive force takes over and causes the cantilever to deflect away from the surface. A laser beam is used to detect cantilever deflections towards or away from the surface. By reflecting an incident beam off the flat top of the cantilever, any cantilever deflection will cause slight changes in the direction of the reflected beam. A position sensitive photo diode (PSPD) can be used to track these changes.

AFM images the topography of a sample surface under interest, which is monitored by the PSPD by use of a feedback loop to control the height of the tip on the surface of interest thus maintaining constant laser position. Hence, the AFM can generate an accurate topographic map of the surface features.

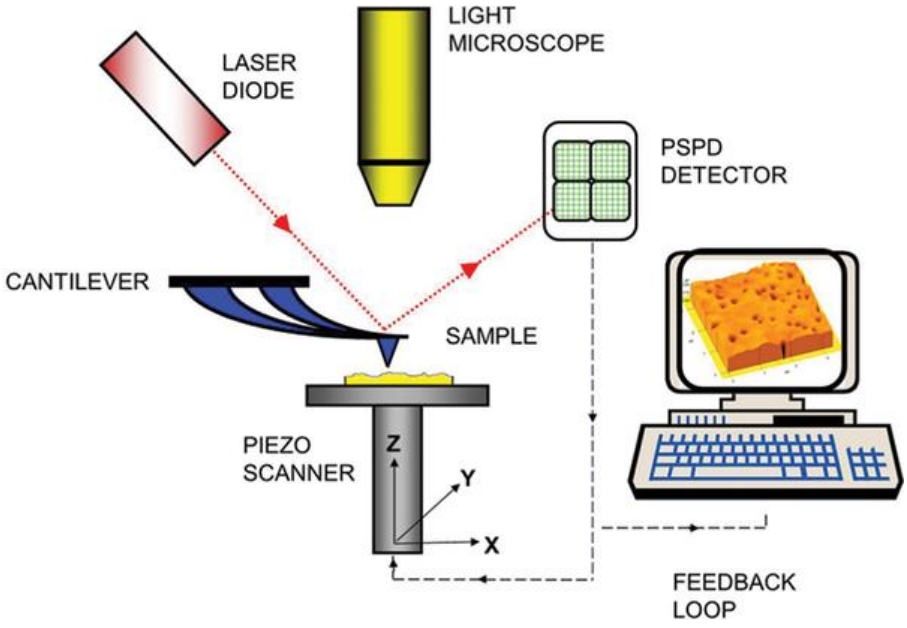


**Figure 21: Schematic of AFM**

### 3.5.5. Working principle of Variable Network Analyzer

Vector Network Analyzer is used to measure the shielding effectiveness of any material. The VNA works on principle of the difference of transmitted and reflected signal across the band of frequency ranges of a material under test. Hence, enables a material to be fully characterized in term of absorption, reflection and multiple reflection losses for attenuation of EM wave. Working process of vector network analyzer operation is represented by (**Figure 22**).

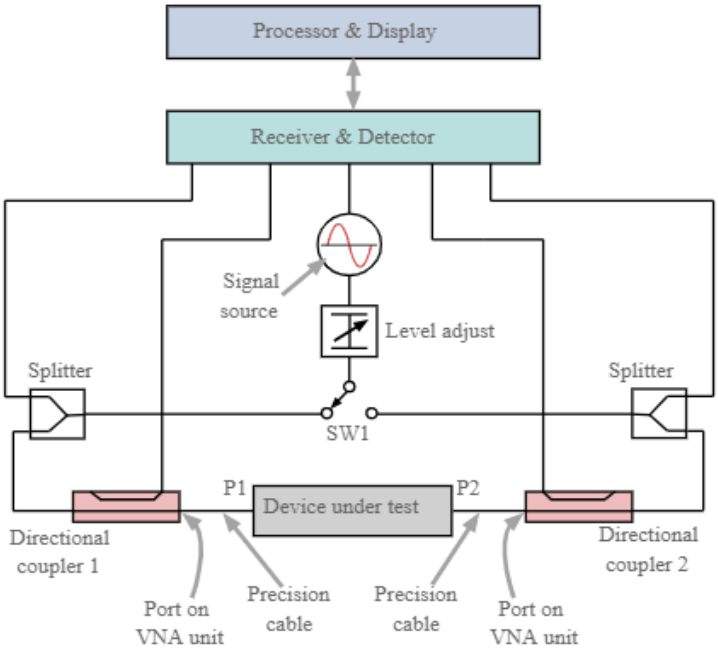


**Figure 22: Block diagram of VNA**

# Chapter 4

# Results & Discussions

Morphological evaluation of nanocomposites was carried out via SEM, FTIR and XRD for identifying the interaction of BNNS and PET.

## 4.1. Dimensional Analysis of BNNS

BNNS used were prepared and characterized by M. Azeem et.al [42]. Current work is a continuation of that work. Dimensional analysis of Boron Nitride Nano sheets was carried out using characterization techniques i.e. AFM and SEM. The SEM and AFM images indicated that lateral dimension of BNNS was around 0.5-1 um. AFM histogram suggests the mean thickness of Nano sheet around 3mm, predicting the no of layers per flake to be around 9-10 (**Figure 23)**.

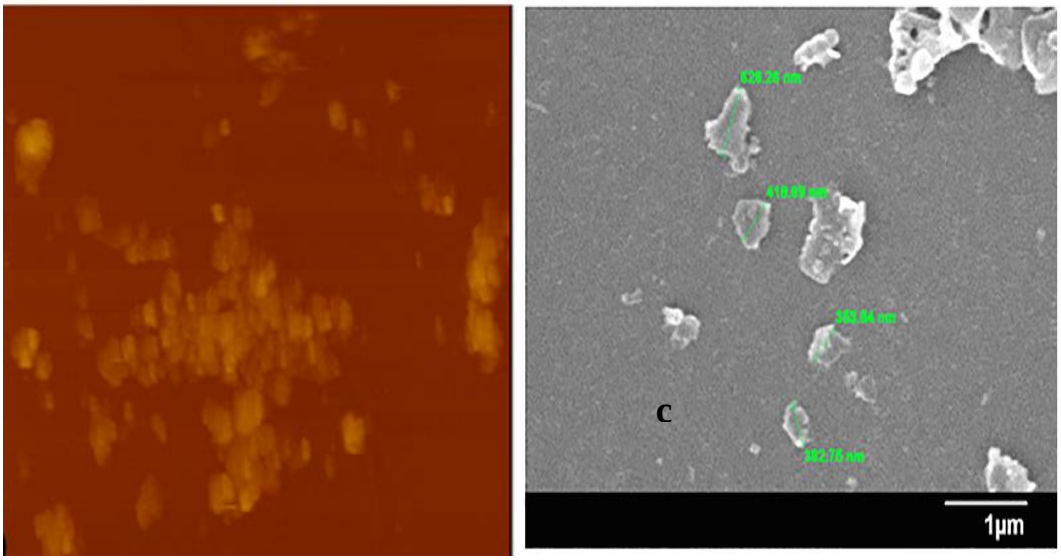


**Figure 23: (a) AFM (b) SEM**

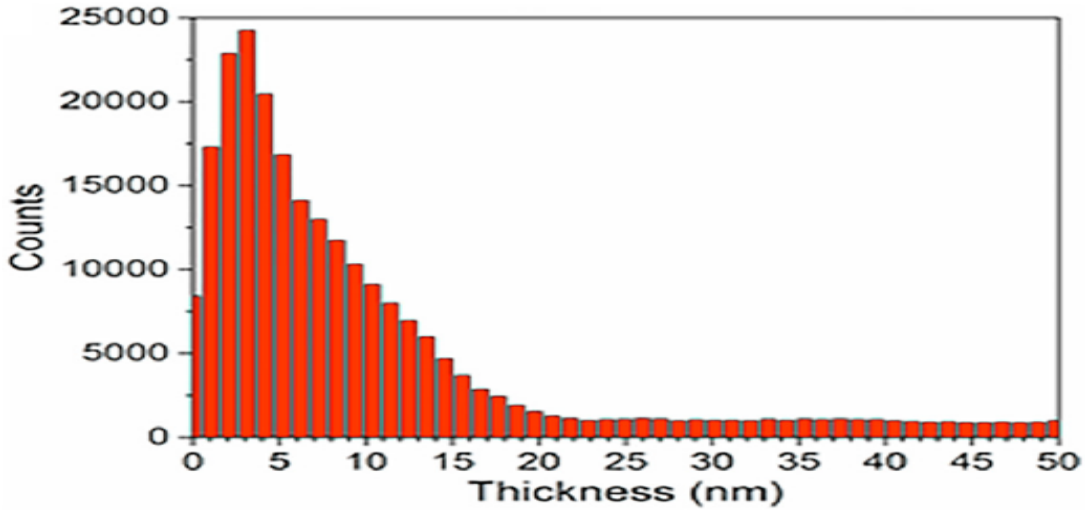


**Figure 24: AFM histogram**

## 4.2. SEM

A porous top and dense bottom surface morphological pattern was depicted in all film samples along with varying proportions. Visually a rough evaporation/top surface stature was observed whereas the bottom surface possesses shinny optics.

### 4.2.1. Rough/Top

A drastic morphological change was observed with increase in concentration of Nano sheets. Pure PET film was totally porous as seen in (**Figure 25**), (**Figure 26-28**) clearly indicates the decrease in porosity with increase in weight % of Nano sheets. Further, decrease in pore size and its distribution can be examined in 0.025wt% composite relative to pure PET film, depicting clear inclusion of Nano sheets. Same trend was observed in all the higher concentration composites and perfect dense structure was exhibited with 0.075wt% of Nano sheets composite. The 0.075wt% of Nano sheets in PET polymer exhibits the perfect dense structure devoid of any pore or cavity but with minor imperfections. Visually, first impression of 0.05wt% composite seems to contain pores, however at higher resolution they were seen to be cavities and not pores **(Figure 29,30)**. It is obvious that the change in morphologies exhibited by samples with higher concentration of Nano sheets is quite remarkable with minor concentration of factors 0.05%-0.075% of PET polymer. It may be highlighted that visually no physical evidence of Nano sheets on the surface was screened the very reason can be usage of the minute content of H-BNN Sheets.

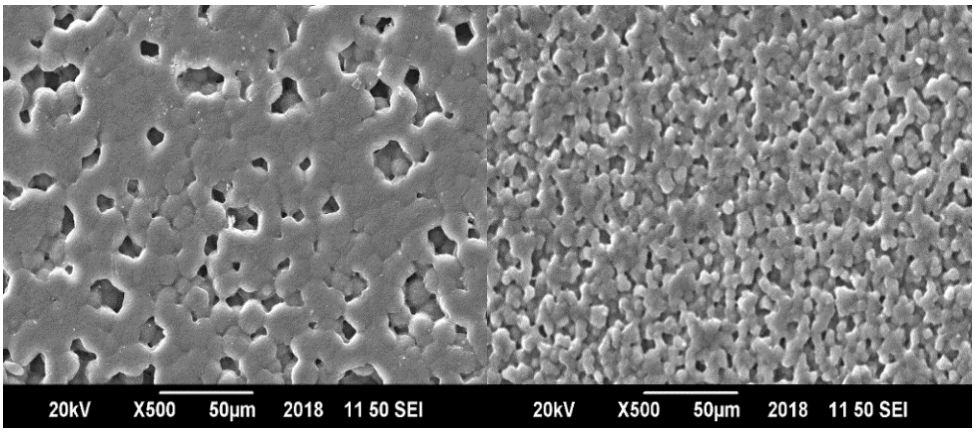


**Figure *25*: Pure PET film-Surface** ***Figure 26: .025wt%-Surface***

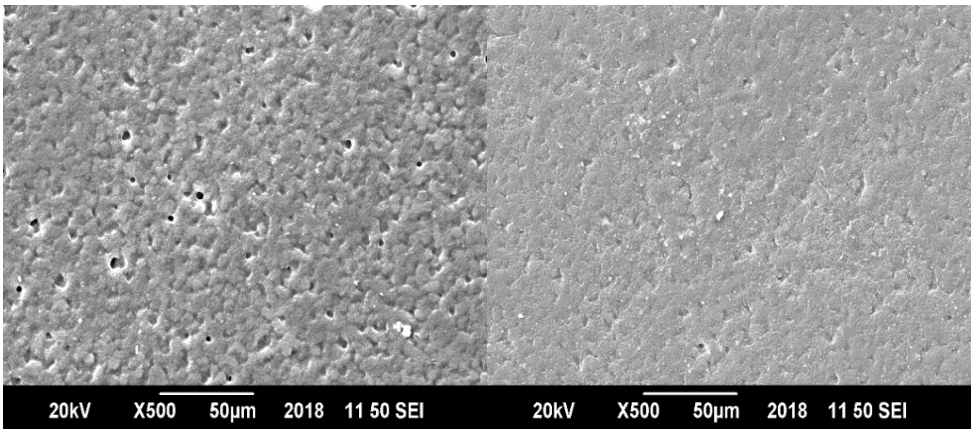


**Figure *27*: .050wt%-Surface** ***Figure 28: .075wt%-Surface-500X***

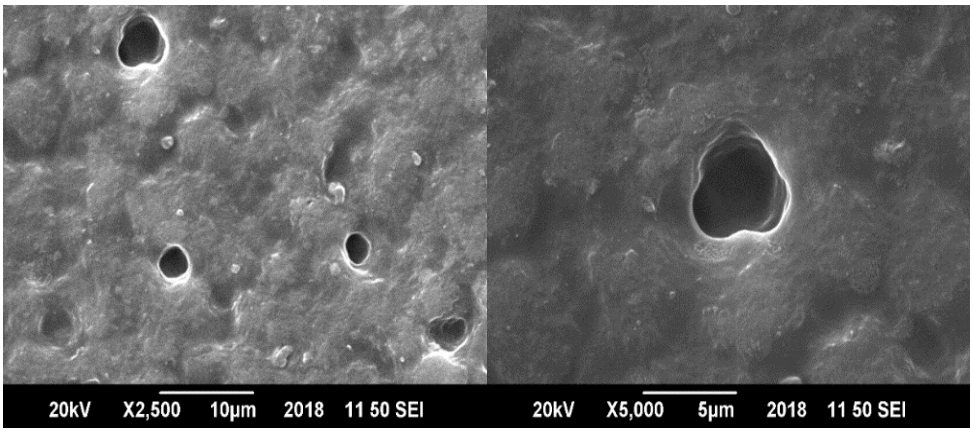


**Figure *29*: .050wt%-2500X** ***Figure 30: .050wt%-X5000***

### 4.2.2 Cross-Section

Self-explanatory and obvious cross-section SEM images were obtained (**Figure 31-34**). Clear transition in the arrangement of polymeric chains can be seen in pure film upon moving from top to bottom in a surface scan of SEM. Similar pattern was observed experimentally in higher wt% composites. In Pure sample, polymer chains at bottom give a dense like appearance with little spacing's in between. However, mid to top portion of cross-section, chains appear to be very slightly tangled containing large pores and voids. 0.025wt% depicts a semi-dense like structure with bottom portion being completely dense and top surface having slight cracks and minute pores. 0.05wt% and 0.075wt% samples exhibit perfectly dense bottom structure and an almost perfect dense top surface. During the drying step of membrane fabrication, solvent evaporates and leaves the gaps which are filled by polymer to a great extent but not entirely, this being the reason for creation of pores as seen in pure sample.

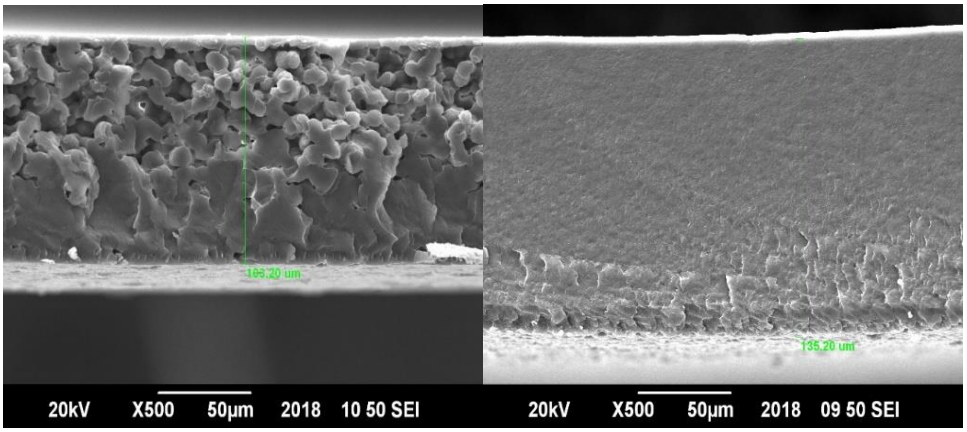


**Figure *31*: Pure-Cross-Section** ***Figure 32: .025wt%-Cross-Section***

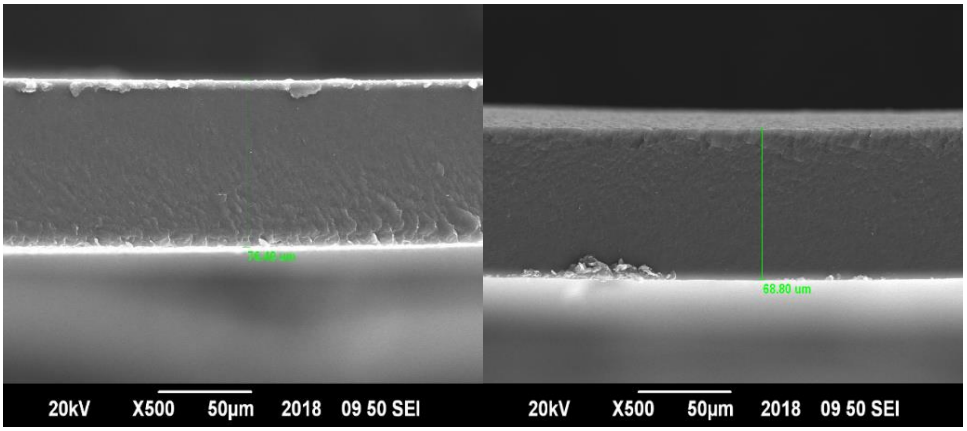


**Figure *33*:050wt%-Cross-Section** ***Figure 34: .075wt%-Cross-Section***

However, in composites, as the solvent evaporates and leaves the gaps, these gaps in polymeric chains are filled mostly by polymer itself and remaining by Nano sheets, thereby generating a dense structure. It may be noted that, as the solvent evaporation is a relatively slow process, during its initial stages most of the polymer settles down at the bottom thus forming a comparably denser structure.

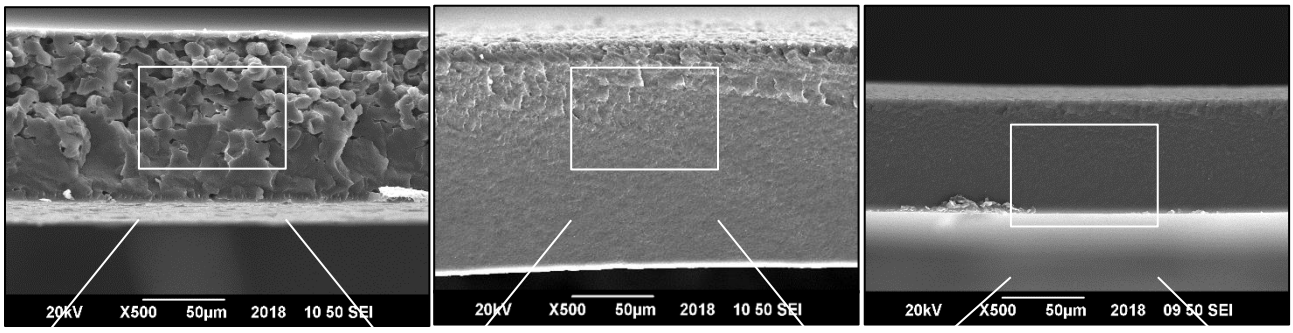

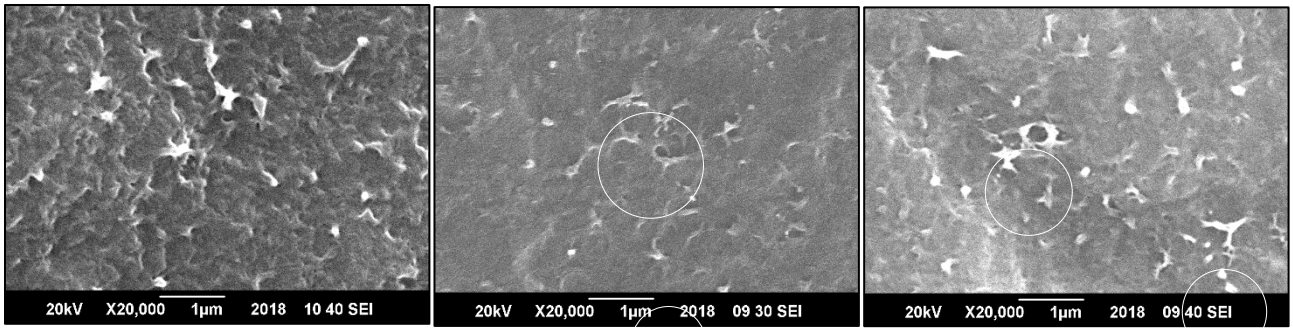


(a) Cross-section-SEM-0wt% PET Film

(b) Cross-section SEM-0.025wt% PET Film

(c) Cross-section SEM-0.050wt% PET Film

**Figure 35: Cross-Section SEM**

Cross sectional view of films via SEM indicated asymmetrical nature of films. Films become more porous moving from shiny/bottom to rough/top surface, also with increase in weight% of BNN sheets the dense side was seen to become further denser and porous / rough sides also become denser. Evaporating surface SEM clearly showed dense structure of all the composites, indicating that Nano sheets had filled the pores and voids and had been successfully incorporated inside the polymer matrix. Furthermore, an interesting interaction of Nano sheets was observed (**Figure 35**), i.e. webbed like structure was formed by Nano sheets, that became more apparent with increase in filler loading.

## 4.3. XRD

### 4.3.1 Nano sheets

XRD technique was applied to confirm the crystal structure of Nano sheets prepared. Characteristic sharp peak of BNNS at 26.75 2θ was obtained for 1500 rpm Nano sheet samples without any impurities as seen in (**Figure 36**) with all sample's d spacing being nearly 0.33nm, which corresponds to the available literature on the current subject. Sharp peaks affirm the assertion that Nano sheets had exfoliated defect free, without losing their crystal structure [43-45]

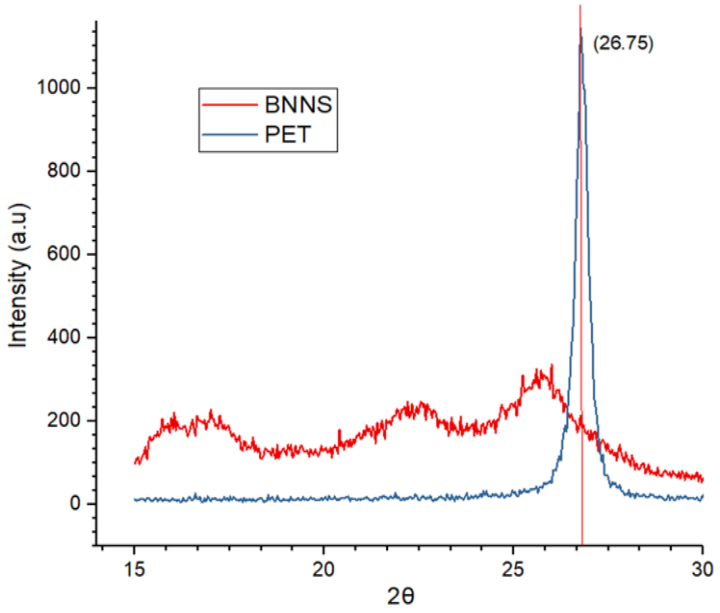


**Figure 36: BNNS and PET polymer combined XRD**

### 4.3.2. Nanocomposites

Characteristic peaks at (17.31-17.9), (22.1-23.07) and at (25.6-26.5) 2θ corresponding to (010), (110) and (100) planes were observed for all samples with varying intensities, indicating that all the samples had retained their crystal structure to varying extents. PET film with zero filler loading exhibited lowest intensity peaks, due to loosening of polymeric chain due to heating treatment at elevated temperatures. An increase in crystallinity can be seen for all composites (**Figure 37**), complementing SEM results and reconfirming that Nano sheets had played a significant role in enhancing chain entanglement thereby increasing crystallinity and consequently decrease in permeation. XRD results of all the samples comply with SEM results. No peak shift was observed for all the composites which indicate the interaction of of h-BN with polymer being strictly physical, however the h-BN peak in Nanocomposites was not very apparent, due to superposition of (100) plane peak of PET with h-BN peak and the fact that the loading of BNNS is very low.

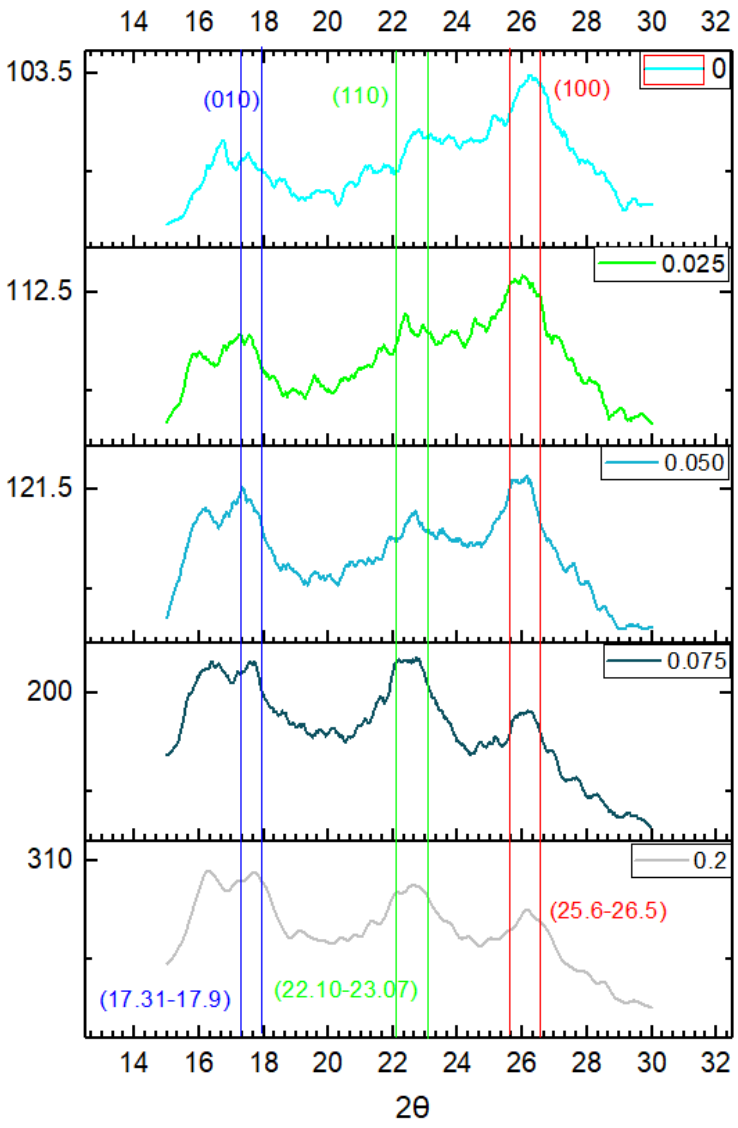


**Figure 37: PET/BNNS nanocomposites XRD**

## 4.4. FTIR

IR of the pure membrane and composite with highest loading were examined for the purpose of finding out the interaction of Nano sheets with the polymer and it was deduced that both the samples contained all the essential peaks and no new peak of any bond that might have been formed if h-BN had reacted with polymer (**Figure 38**).

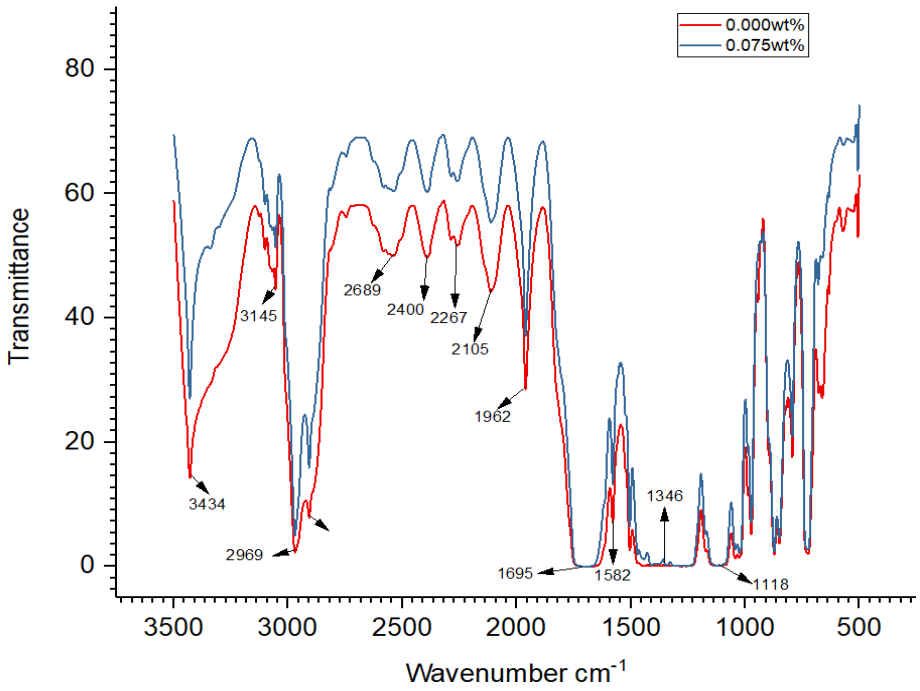


**Figure 39: PET/BNNS Nanocomposite FTIR comparison with zero loading film**

## 4.5. Tensile Testing

To investigate the effect of Nano sheets on mechanical properties, tensile strength tests were conducted adhering to the ASTM D8808-2. An increasing trend in tensile strength was depicted by all the samples, an increase of 23.3% for the 0.2wt% composite was seen hence reaffirming the reinforcement abilities of BNNS. Noticeably large amount of elongation-at-break was observed in all the composites compared to the pure film, which is peculiar when considering that most fillers cause a reduction in elongation-at-break and consequently enhance modulus, the present behavior may be attributed to the web like structured form by Nano sheets inside polymer matrix as observed in SEM images thereby making composites comparatively more ductile. Also, suppression of stress induced crystallization in PET/h-BN composites could be another possible cause of enhanced ductility (**Figure 39-41**).

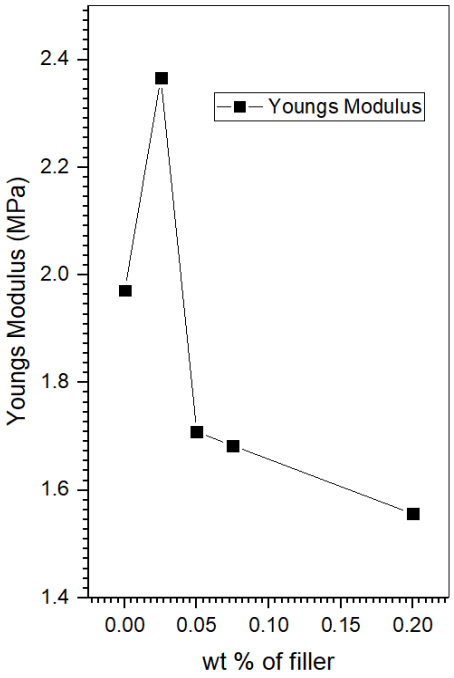


**Figure 40: Young's Modulus variation with increase in filler loading**

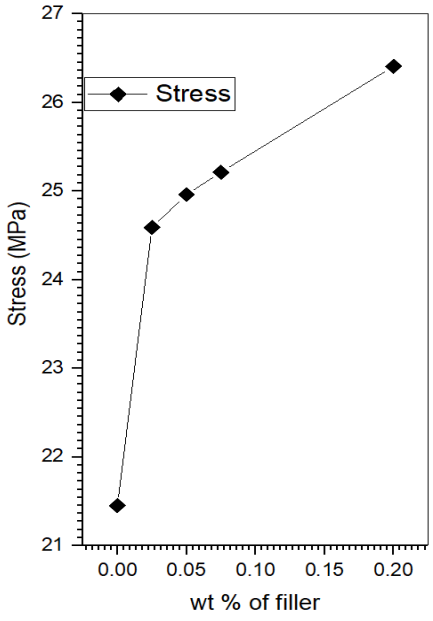


**Figure 41: Stress variation with increase in filler loading**

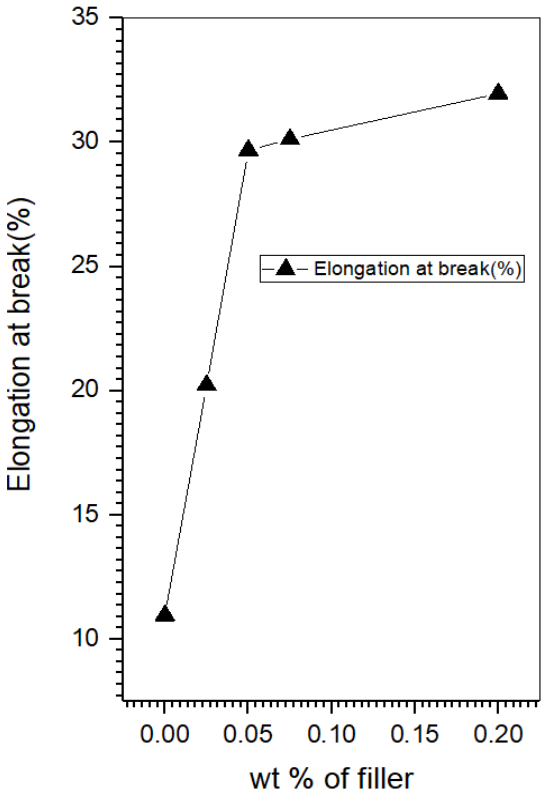


**Figure 42: Elongation Break variation with increase in filler loading**

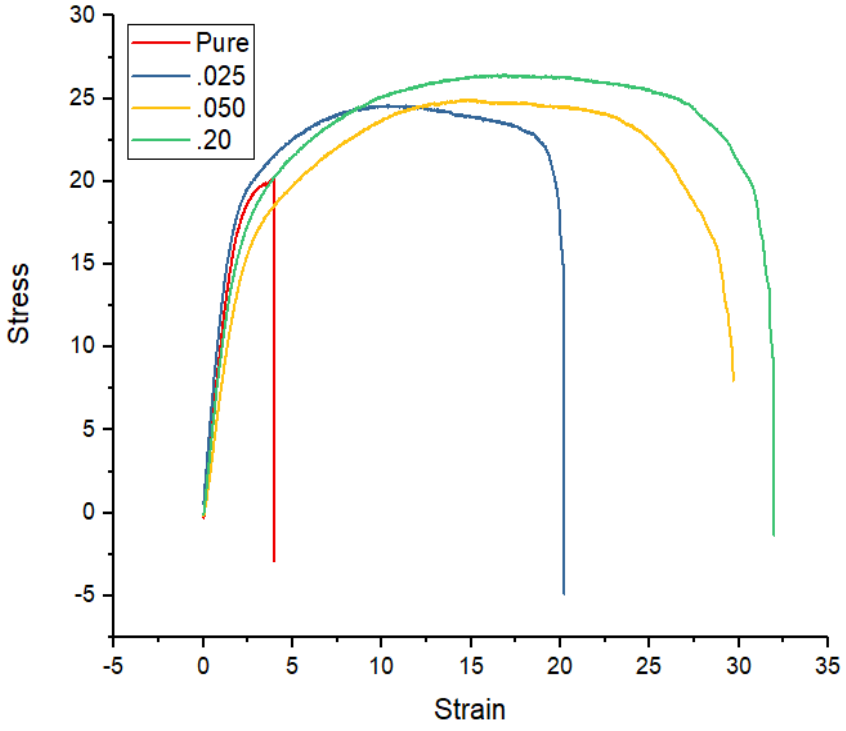


**Figure 43: Stress Strain Curve for PET/BNNS Nanocomposites**

## 4.6. EMI Shielding effectivess

EMI shielding effectiveness test was carried out by keeping in mind mainly three contributing factors i.e. Shielding effectiveness due to reflection, Shielding effectiveness due to absorption and Shielding effectiveness due to multiple reflection. Shielding effectiveness due to multiple reflection exist only in thin materials where thickness lies in nm-um range. However, the materials in the range of mm possess attenuation only due to reflection or absorption. Our samples of PET and H-BNN composites have thickness of .1mm. Therefore, we will look in to only two factors responsible for loss of EM wave i.e. reflection loss (dB) and absorption loss (dB).

### 4.6.1. Shielding effectiveness by Reflection loss SE(R)

A preliminary factor to estimate shielding effectiveness due to reflection loss SE(R) depends on following factors:

δ: Conductivity of material

f: Frequency of EM wave

μ: Permeability of material

Therefore the relation for reflection loss can be represented as:

$SER(dB) = 39.5 + 10\log(\frac{\delta}{2\Pi f\mu})$ : Value of reflection loss varies from frequency to frequency

### 4.6.2. Shielding effectiveness by Absorption loss SE (A)

The second contributing factor to estimate shielding effectiveness is absorption of EM wave. The absorption of EM wave in a medium is dependent on:

δ: Conductivity of material

f: Frequency of EM wave

μ: Permeability of material

d: Thickness of material

Therefore the relation that holds the quantification of absorption loss in medium is represented in the form:

$SEA(dB) = 8.7d\sqrt{2\Pi f\mu}$ : Value of absorption loss also varies from frequency to frequency.

### 4.6.3. Reflection loss SE(R) in Pure PET

PET polymer is basically an insulating polymer; reflection phenomenon is basically the main contributing factor for attenuation of incident EM wave and also center of interest for all researchers. Further, as obvious value of shielding effectiveness varies with frequency. Therefore, response of shielding effectiveness due to reflection at low frequency range is different as compared to attenuation of EM wave due to reflection at high frequency ranges. EMI shielding effectiveness achieved in pure PET in KHz, MHz and GHz frequency ranges is depicted in graphs below:

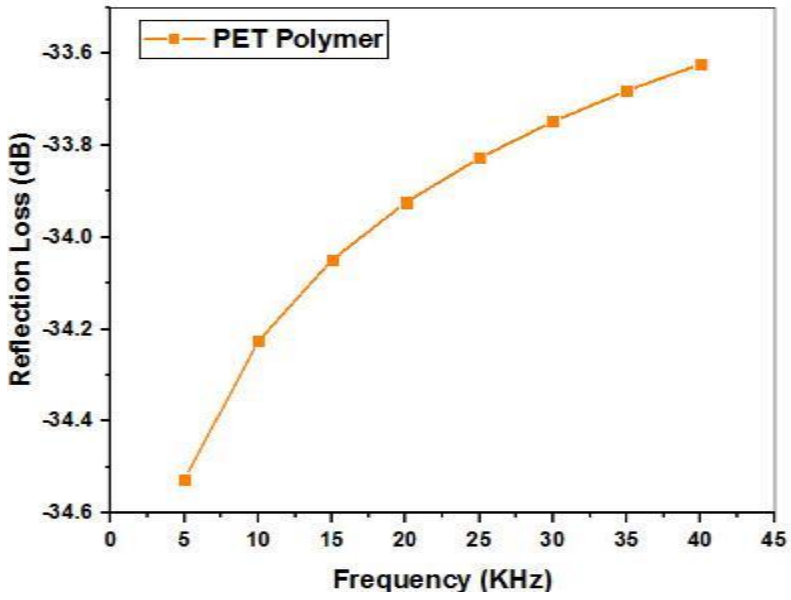


**Figure 44: Shielding effectiveness of pure PET in KHz due Reflection loss**

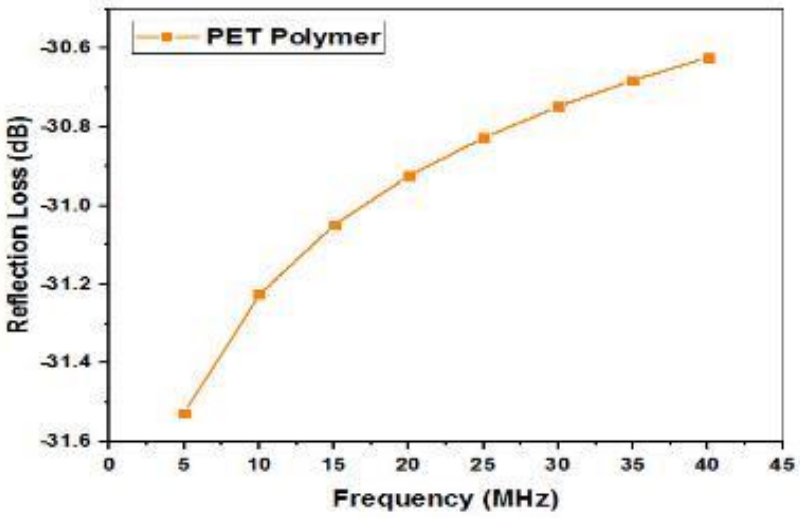


**Figure 45: Shielding effectiveness of pure PET in MHz due Reflection loss**

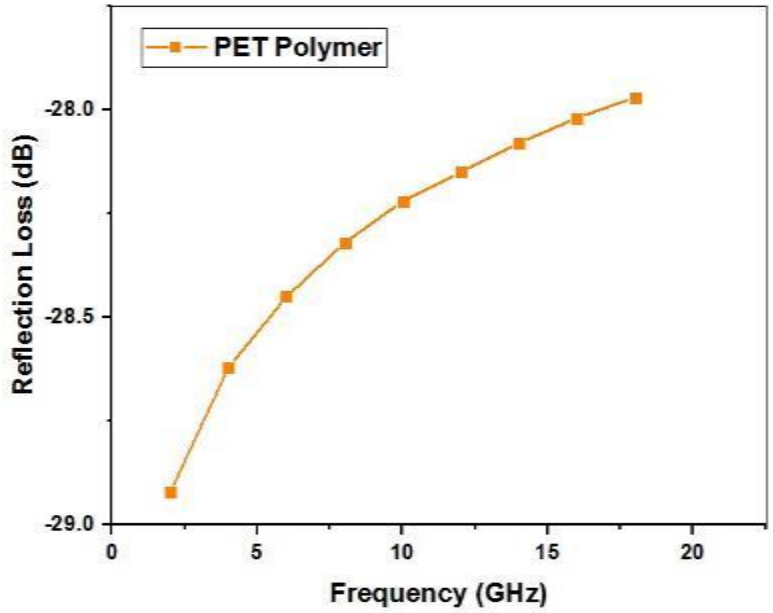


**Figure 46: Shielding effectiveness of pure PET in GHz due Reflection loss**

### 4.6.4. Reflection loss SE(R) in PET Nanocomposite

Addition of Hexagonal Boron Nitrate Nano sheets not only enhanced the strength of PET but also make it more suitable for attenuation in even GHz frequency range. It was observed that due addition of Nano Sheets in PET polymer, the attenuation of EM waves though remains in between 30-40 dB in KHz, MHz and GHz, but with enhanced adhesion and tensile strength. The

attenuation behavior of incident EM wave at different frequency ranges has been elaborated explicitly in 03 Graphs.

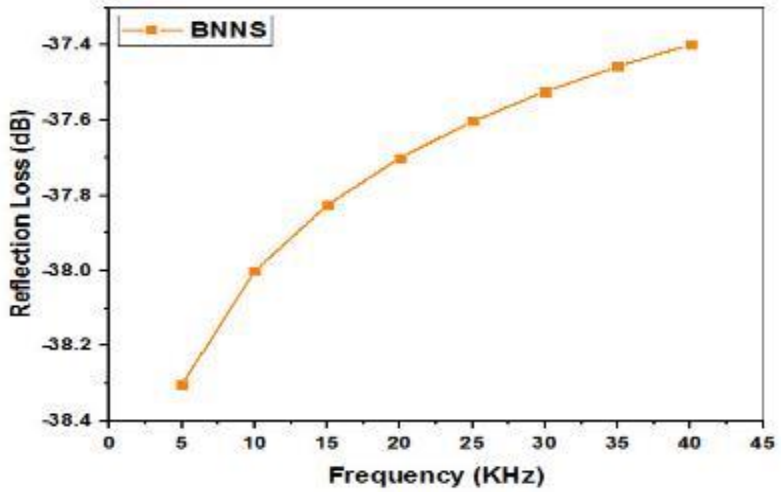


**Figure 47: Shielding effectiveness of PET Nanocomposite in KHz due Reflection loss**

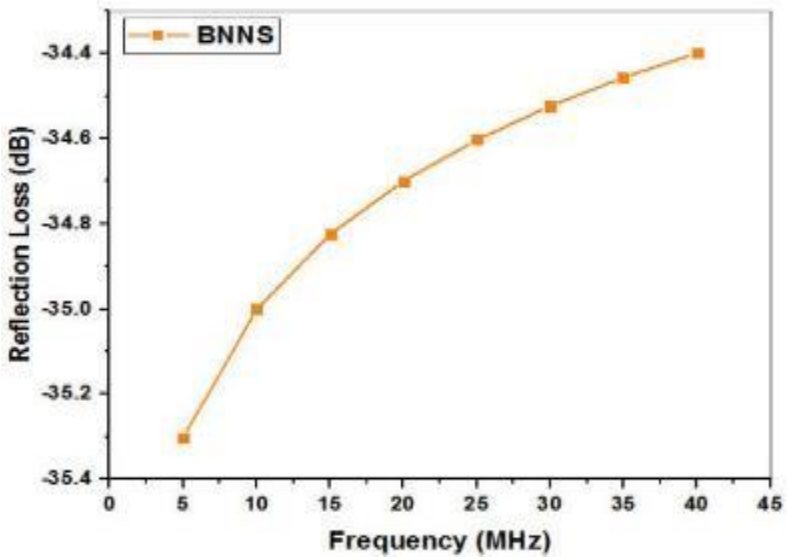


**Figure 47: Shielding effectiveness of PET Nano composite in MHz due reflection loss**

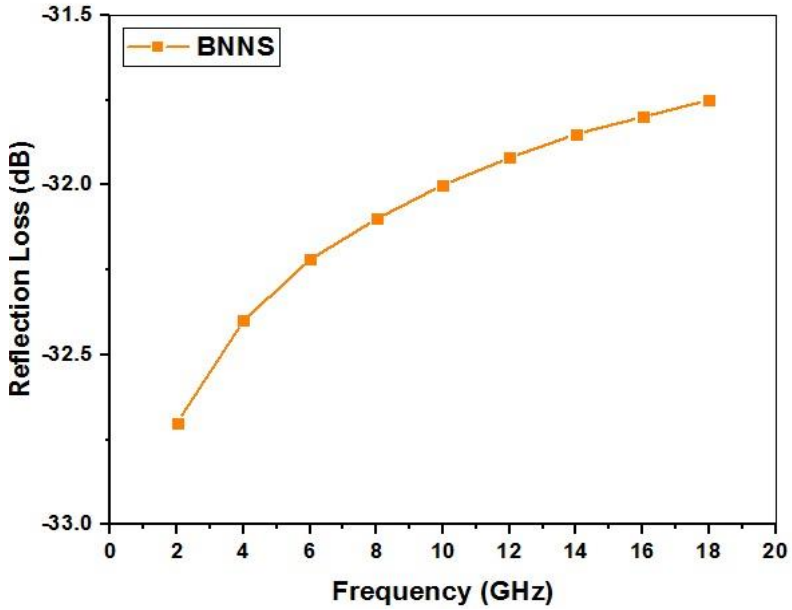


**Figure 48: Shielding effectiveness of PET Nano composite in GHz due reflection loss**

# Chapter 5

# Conclusion

Main objective of the above research was to focus on development of economical and reliable EMI shielding material particularly for Missile systems and generally for Military equipments. Fabrication challenges in EMI shielding materials were several. Initially only PET polymer was synthesized in N-Methyl-2-Pyrrolidone (NMP) and observed that attenuation of incident EM wave exists due to reflection loss, however, tensile strength is less. Later, to enhance the tensile strength and attenuation of EM wave for wide frequency ranges, hexagonal boron nitrate Nano sheets were added in PET polymer with various loading 0.01wt%, 0.05wt% and 0.075wt% to fabricate a PET Nanocomposite material. Tensile strength testing, which was the significant characterization technique for this research showed quite encouraging results in favor of Nano sheets, depicting its superior tensile strength as compared to pure PET polymer. Ibid research work help us to analyze that the results achieved are good enough for Military systems and the PET nanocomposites are considered the suitable option of EMI attenuation in GHZ frequency range for Military applications.

# Chapter 6

# Future Recommendations

PET-BNNS films were tested for their EMI shielding properties in KHz, MHz and GHz ranges and compared with pure PET films. It was observed that pure PET film showed significant attenuation of EM wave but less tensile strength. Further, PET Nanocomposites have resolved both issues of strength as well as attenuation of incident of EM wave for Military applications, attenuation values are in the range of 30-40 dB. It is emphasized that Gaps for better attenuation of EM shielding still exists. Therefore, use of polymers having both reflection and absorption properties can considerably enhance the EMI effectiveness of a material, for this purpose even the mixture of both Graphene and Hexagonal Boron Nitride can be explored for achieving dual effect for better shielding effectiveness.

# References

[1] EMI Shielding: Methods and Materials—A Review: S. Geetha,K. K. Satheesh Kumar, Chepuri R. K. Rao, M. Vijayan, D. C. Trivedi

[2] Violette, J. L. N.; White, D. R. J.; Violette, M. F. Electromagnetic Compatibility Handbook; Van Nostrand Reinhold Company:New York, 1987.

[3] Jang, J. O.; Park, J. W. U.S. Pat 6,355,707 B1 (2002).

[4] Miller, H. K. Mater Eval 1997, 55, 994.

[5] Sienkiewicz, Z. Power Eng J 1998, 12, 131.

[6] Tech. Trends III—International Reports on Emerging Technologies—EMI Shielding, Conductive Plastics and Elastomers; Innovation: S.A. Paris, 1987; p 128

[7] M. C. Ribadeneyra, J. P. de Diego and M. G. Gonz´alez, PhD thesis, Universidad Carlos III de Madrid, 2014.

[8] J. Wang, J. Wang, B. Zhang, Y. Sun, W. Chen and T. Wang, J.Magn. Magn. Mater, 2016, 401, 209–216.

[9] F. Meng, H. Wang, F. Huang, Y. Guo, Z. Wang, D. Hui and Z. Zhou, Composites, Part B, 2018, 137, 260–277.

[10] J. Liu, W.-Q. Cao, H.-B. Jin, J. Yuan, D.-Q. Zhang and M.-S. Cao, J. Mater. Chem. C, 2015, 3, 4670–4677.

[11] G. G. Bush, J. Appl. Phys., 1988, 63, 3765–3767.

[12] Lightweight Electromagnetic Interference Shielding Materials and Their MechanismsLiying Zhang, Shuguang Bi and Ming Liu

[13] Yang YL, Gupta MC. Novel carbon nanotube-polystyrene foam composites for electromagnetic interference shielding. Nano Letters. 2005; 5:2131-2134

[14] Crooks LE. Noise reduction techniques in electronic systems (2nd ed.), Henry W. Ott. Wiley-Interscience: New York. 1988. Magnetic Resonance in Medicine. 1989; 10:426-427

[15] M. C. Ribadeneyra, J. P. de Diego and M. G. Gonz´alez, PhD thesis, Universidad Carlos III de Madrid, 2014

[16] D. L. Leslie-Pelecky and R. D. Rieke, Chem. Mater., 1996, 8, 1770–1783.

[17] X. Zhang, P. Guan and X. Dong, Appl. Phys. Lett., 2010, 97, 033107.

[18] R. Dosoudil, M. Usakova, J. Franek, J. Slama and A. Gruskova, IEEE Trans. Magn., 2010, 46, 436–439.

[19] A. Habib, S. Xu, E. Walker, M. Ondeck, R. Swaminathan and M. McHenry, J. Appl. Phys., 2012, 111, 07B305.

[20] R. Kodama, J. Magn. Magn. Mater. 1999, 200, 359–372.

[21] Review of electromagnetic interference shielding materials fabricated by iron ingredients: Vineeta Shukla: Nanoscale Adv., 2019, 1, 1640

[22] Y. Liu, S. Wei, B. Xu, Y. Wang, H. Tian and H. Tong, J. Mag. Mater. 2014, 349, 57–62.

[23] H. Lv, G. Ji, M. Wang, C. Shang, H. Zhang and Y. Du, RSC Adv., 2014, 4, 57529–57533.

[24] P. Saini and M. Arora, in New Polymers for Special Applications, InTech, 2012.

[25] Y. Li, M. Yu, P. Yang and J. Fu, Ind. Eng. Chem. Res., 2017, 56, 8872–8879.

[26] YIN Chun, STARK Brandon, and CHEN Yangquan, et al. Adaptive minimum energy cognitive lighting control: integer order vs fractional order strategies in sliding mode based extremum seeking Mechatronics [J].Mechatronics, October 2013, Volume 23, Issue 7, pp 863-872.

[27] ZHANG Xiaoyi, AN Zhentao, YAN Jun. Research Progress of Electromagnetism Shielding Fabric [J].Packaging Engineering, 2014, 35(3): 102-106

[28] Electromagnetic interference shielding effectiveness of carbon Materials D.D.L. Chung* Composite Materials Research Laboratory, State University of New York at Buffalo, Buffalo, NY 14260-4400, USA Received 23 March 2000; accepted 22 July 2000.

[29] Composite Materials for Electromagnetic Interference Shielding Pavel Steffan, Jiri Stehlik, Radimir Vrba

[30] Preparation and Study of Electromagnetic Interference Shielding Materials Comprised of Ni-Co Coated on Web-Like Biocarbon Nanofibers via Electroless Deposition Xiaohu Huang, Bo Dai, Yong Ren, Jing Xu, and Pei Zhu.

[31] Hybrid Nanocomposite Material for EMI Shielding in Spacecrafts Article in Advanced Materials Research · April 2015

[32] EMI shielding using composite materials with two sources magnetron sputtering: J Ziaja et al 2016 IOP Conf. Ser.: Mater. Sci. Eng. 113 012010

[33] Composite materials for electromagnetic shielding Article · January 2016.

[34] Detection of electromagnetic interference shielding effect of Hanji mixed with carbon nanotubes using nuclear magnetic resonance techniques Young Seok Byun1,2, Shin Ae Chae1, Geun Yeong Park3, Haeseong Lee3,♠ and Oc Hee Han1,2,4,.

[35] Fabrication of Flexible, Lightweight, Magnetic Mushroom Gills and Coral-Like MXene–Carbon Nanotube Nanocomposites for EMI Shielding Application: Kanthasamy Raagulan 1 , Ramanaskanda Braveenth 1 , Lee Ro Lee 1, Joonsik Lee 2, Bo Mi Kim 3, Jai Jung Moon 4, Sang Bok Lee 2,* and Kyu Yun Chai 1,

[36] Room-Temperature Ferromagnetic Sr3YCo4O10+δ and Carbon Black-Reinforced Polyvinylidenefluoride Composites toward High- Performance Electromagnetic Interference Shielding Vidhya Lalan,† Aparna Puthiyedath Narayanan,‡ Kuzhichalil Peethambharan Surendran,‡ and Subodh Ganesanpotti

[37] Comparison of Experimental and Modeled EMI Shielding Properties of Periodic Porous XGNP/PLA Composites Avi Bregman 1, Eric Michielssen 2 and Alan Taub.

[38] Handbook of Electrochemistry, 2007 by Santosh K .Haram

[39] Basic Theory of Magnetron sputtering by Feng Shi 27th July 2018

[40] Fu S.Y., Feng X.Q., Lauke B., and Mai Y.W., Composites part B: Engineering, vol. 39, 2008, pp. 933

[41] Picard, etal., Barrier properties of nylon 6-montmorillonite nanocomposite membranes prepared by melt blending: influence of the clay content and dispersion state: consequences on modelling. 2007. **292**(1-2): p. 133-144

[42] Azeem, M., et al., Improving gas barrier properties with boron nitride nanosheets in polymer-composites. 2019. **12**: p. 1535-1541.

[43] Ko, W.Y., et al., Fabrication of Hexagonal Boron Nitride Nanosheets by Using a Simple Thermal Exfoliation Process. 2016. **63**(3): p. 303-307.

[44] Huang, C., et al., Stable colloidal boron nitride Nanosheet dispersion and its potential application in catalysis. 2013. **1**(39): p. 12192-12197.

[45] Li, L.H., et al., High-efficient production of boron nitride Nanosheets via an optimized ball milling process for lubrication in oil. 2014. **4**: p. 7288